Dispensing-Based Bioprinting of Hybrid Scaffolds with Vessel-like Channels for Tissue Engineering Applications – A Brief Review

Saman Naghieh, MD Sarker, Mohammad Izadifar, Xiongbiao Chen

PII: S1751-6161(17)30525-8
DOI: http://dx.doi.org/10.1016/j.jmbbm.2017.11.037
Reference: JMBBM2594

https://www.sciencedirect.com/science/article/pii/S1751616117305258

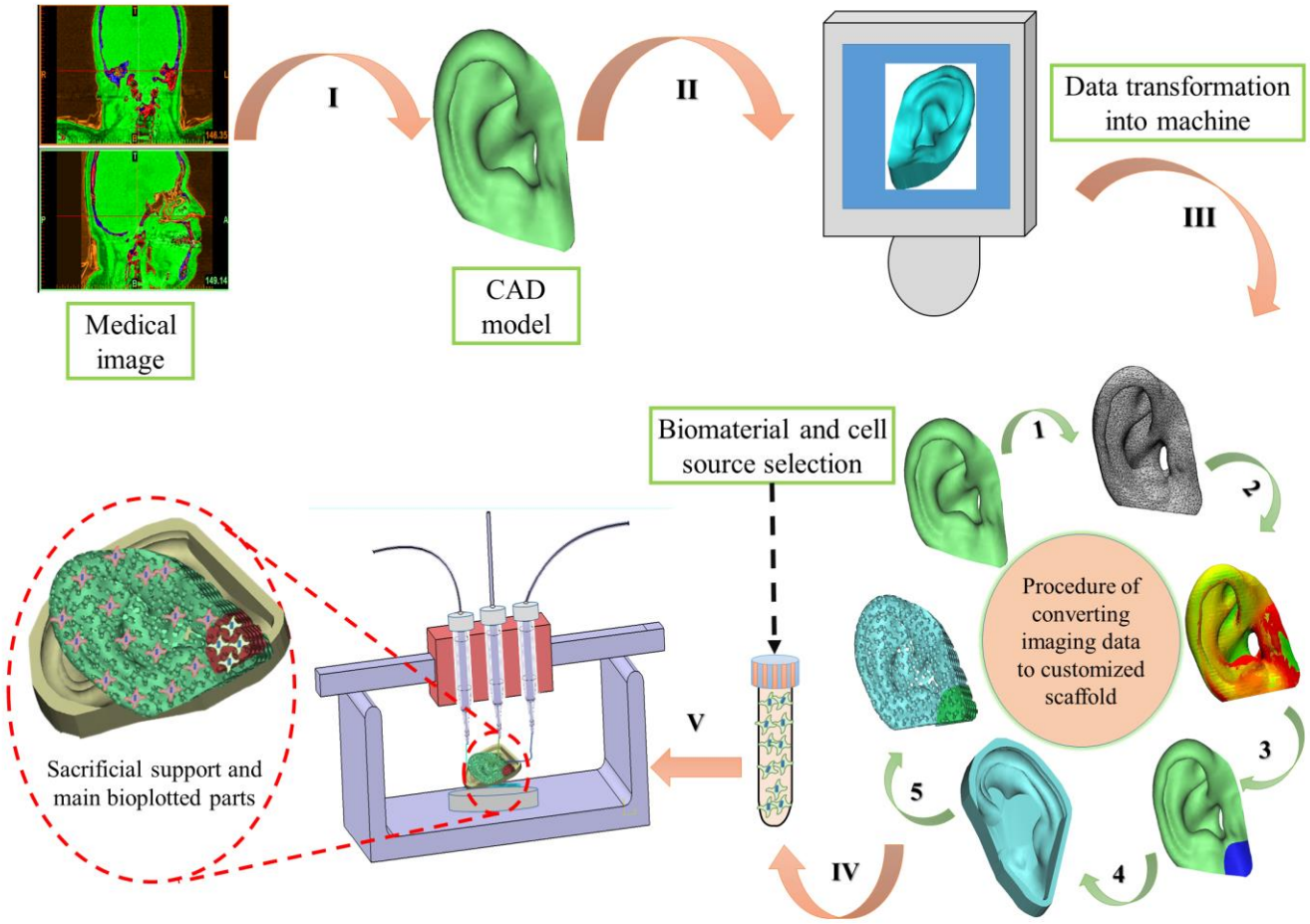

Dispensing-Based Bioprinting of Hybrid Scaffolds with Vessel-like Channels for Tissue Engineering Applications – A Brief Review

Saman Naghieh[1,*]

(san908@mail.usask.ca, Tel.: 001-306-966-5435, Fax: 001-306-966-5427)

MD Sarker[1]

(mas921@mail.usask.ca, Tel.: 001-306-966-5435, Fax: 001-306-966-5427)

Mohammad Izadifar[1,2, 3]

(mohammad.izadifar@usask.ca, Tel.: 001-306-966-5435, Fax: 001-306-966-5427)

Xiongbiao Chen[1,3]

(xbc719@mail.usask.ca, Tel.: 001-306-966-1267, Fax: 001-306-966-5427)

[1]Division of Biomedical Engineering, College of Engineering, University of Saskatchewan, Saskatoon, SK, Canada

[2]Department of Surgery, College of Medicine, University of Saskatchewan, Saskatoon, SK, Canada

[3]Department of Mechanical Engineering, College of Engineering, University of Saskatchewan, Saskatoon, SK, Canada

[*] Corresponding author at: Division of Biomedical Engineering, College of Engineering, University of Saskatchewan, Saskatoon, SK, Canada.

Email address: san908@mail.usask.ca, Tel: +1 306 966 5435 (S. Naghieh).

Abstract

Over the past two decades, significant progress has been achieved in the field of tissue engineering (TE) to restore/repair damaged tissues or organs and, in this regard, scaffolds made from biomaterials have played a critical role. Notably, recent advances in biomaterials and three-dimensional (3D) printing have enabled the manipulation of two or more biomaterials of distinct, yet complementary, mechanical and/or biological properties to form so-called hybrid scaffolds mimicking native tissues. Among various biomaterials, hydrogels synthesized to incorporate living cells and/or biological molecules have dominated due to their hydrated tissue-like environment. Moreover, dispensing-based bioprinting has evolved to the point that it can now be used to create hybrid scaffolds with complex structures. However, the complexities associated with multi-material bioprinting and synthesis of hydrogels used for hybrid scaffolds pose many challenges for their fabrication. This paper presents a brief review of dispensing-based bioprinting of hybrid scaffolds for TE applications. The focus is on the design and fabrication of hybrid scaffolds, including imaging techniques, potential biomaterials, physical architecture, mechanical properties, cell viability, and the importance of vessel-like channels. The key issues and challenges for dispensing-based bioprinting of hybrid scaffolds are also identified and discussed along with recommendations for future research directions. Addressing these issues will significantly enhance the design and fabrication of hybrid scaffolds to and pave the way for translating them into clinical applications.

Keywords

3D bioprinting; Dispensing-based bioprinting; Hybrid scaffolds; Biomaterials; Vessel-like channels; Tissue engineering

1. Introduction

The unavailability of adequate organs to meet the increasing demand for organ transplantation has created a global organ shortage crisis (Kang et al., 2016). Tissue engineering (TE) has emerged as a promising approach to regenerate human tissues and organs. In particular, scaffold-based TE aims to develop cell-seeded micro-constructs, so called 'scaffolds', to eventually replace, protect, restore, or repair damaged tissues such as skin, bladder, trachea, and myocardium after implantation (Atala et al., 2006; Boucard et al., 2007; Cebotari et al., 2006; Langer, 2009; Macchiarini et al., 2008; Matsumura et al., 2003; Sekine et al., 2006). Driving significant innovations in TE, three-dimensional (3D) printing, also known as 'additive manufacturing' (AM), has enabled the creation of biocompatible 3D scaffolds with a wide range of complexities that are suitable for transplantation. The 3D-printed scaffolds should resemble the biological and mechanical properties of native tissue to promote successful and functional tissue regeneration as well as avoid postoperative complications (Boccardi et al., 2015; Teo et al., 2006). To this end, numerous efforts have been made to fabricate biomimetic 3D scaffolds with biological and mechanical properties similar to native tissues.

3D scaffolds can be prepared by both conventional and modern techniques. Conventional methods include electrospinning (Kishan et al., 2016), freeze-drying, gas foaming (Offeddu et al., 2016), and particle or porogen leaching (Kim et al., 2008). Unlike conventional methods, modern techniques such as laser-assisted, inkjet-based, and dispensing-based (also known as extrusion-based) cell printing (Dababneh and Ozbolat, 2014; Murphy and Atala, 2014; Seol et al., 2014; Wang et al., 2016) enable precise control for adding complex features to the scaffolds layer-by-layer as per a virtual computer-aided design (CAD) drawing (Sarker and Chen, 2017). Figure 1 presents schematic diagrams of AM techniques.

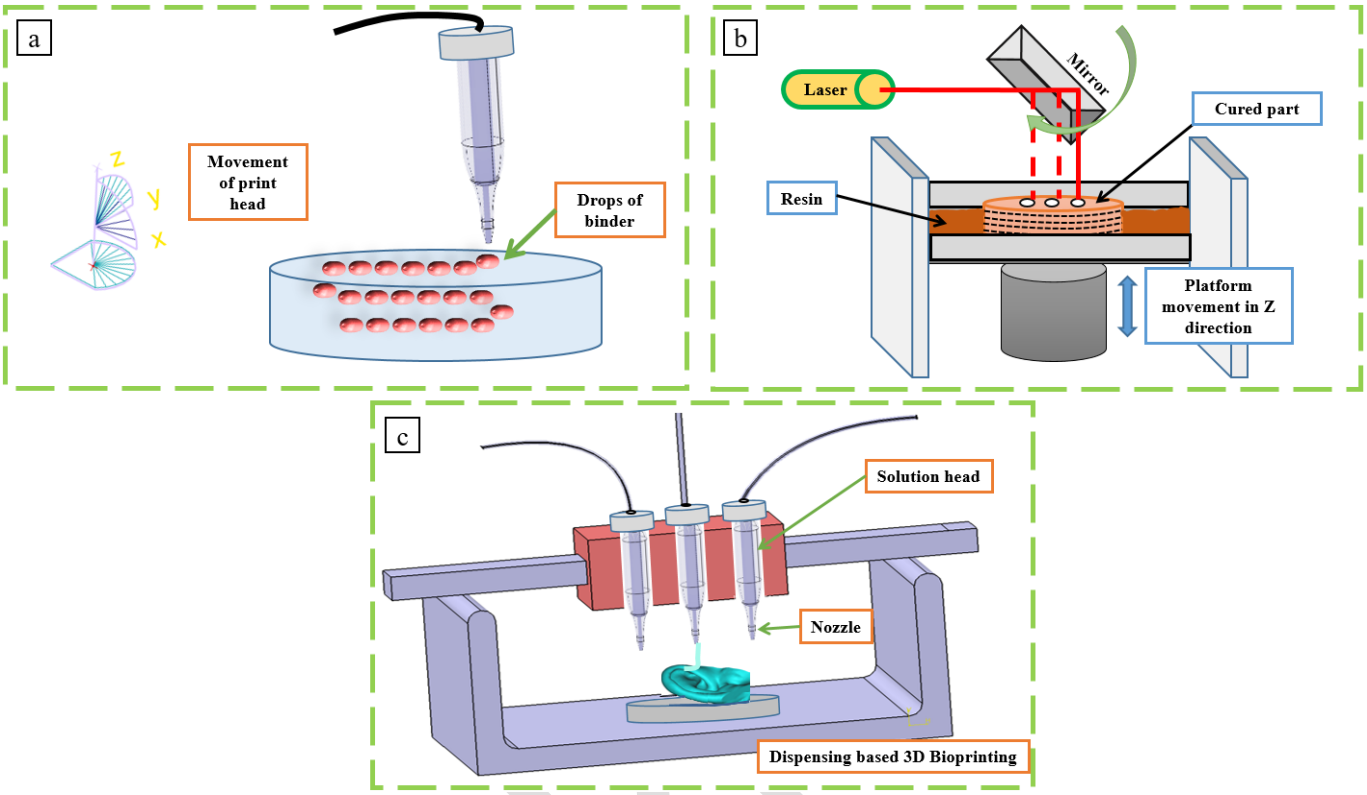

Figure 1. Schematic of a) inkjet-based, b) laser-based, and c) dispensing-based machines

AM techniques are able to fabricate cell-laden hydrogels (Ning and Chen, 2017; Wilson and Boland, 2003) and they facilitate the direct printing of cells or bioactive molecules in defined locations with high cell viability to mimic the targeted tissue (Cui et al., 2012; Fedorovich et al., 2011b; Guillemot et al., 2010; Liu et al., 2010; T. Xu et al., 2012). Table 1 presents the advantages and disadvantages of three AM techniques for TE applications.

Table 1. Merits and demerits of common 3D bioprinting techniques (Guillotin et al., 2010; Hon et al., 2008; Moon et al., 2009; Ozbolat and Yin Yu, 2013; Xu et al., 2013; Yu et al., 2013)

Techniques	**Laser-assisted**	**Inkjet-based**	**Dispensing-based**
Advantages	Nozzle-free technique Printability of viscous biomaterials Good resolution and accuracy No clogging	Good cell viability Printing various cell types Noncontact nozzle Relatively high-resolution printing	Good mechanical properties Shorter fabrication time than the other two methods Printing various concentrations of biomaterials with high cell densities

Disadvantages	Poor mechanical properties and long fabrication time using some biomaterials Cell damage due to using laser	Poor mechanical properties High viscosity biomaterials are not printable Nozzle clogging	Poor cell viability due to shear stress in nozzle Limited resolution, nozzle clogging

Among these three techniques, dispensing-based bioprinting offers the most attractive features. It is less expensive than inkjet- and laser-based printing modules and operationally more flexible with respect to printing multiple materials and cell types for organ printing (Huang et al., 2013; S. Li et al., 2009a, 2009b; Sui et al., 2009; Wang et al., 2015, 2013, 2010; Wang and Xu, 2010). Time pressure, rotary screw, or positive displacement are the main mechanisms in a dispensing-based cell printing system (Figure 2) (M. G. Li et al., 2009). Encapsulated cells, growth factors, proteins, and peptides can be simultaneously dispensed via this technique to form 3D structures (Wang et al., 2006; Xu et al., 2010, 2009, 2007, Yan et al., 2005a, 2005b; Zhang et al., 2007). Over the last decade, this technique has created new opportunities to achieve the goal of complex organ printing (Albrecht et al., 2016; Liu et al., 2015; Wang, 2015; Xu and Wang, 2015; Zhao et al., 2014; Zhao and Wang, 2013; Zhou et al., 2016), so that the first efforts to print large-scale 3D constructs have been made using this technique. In 2007, the dispensing-based bioprinter technique was used to fabricate organs with more than two cell types (Xu et al., 2007). Specifically, adipose tissue-derived stem cells and hepatocytes were assembled into vascular liver tissues using this technique (Wang et al., 2016).

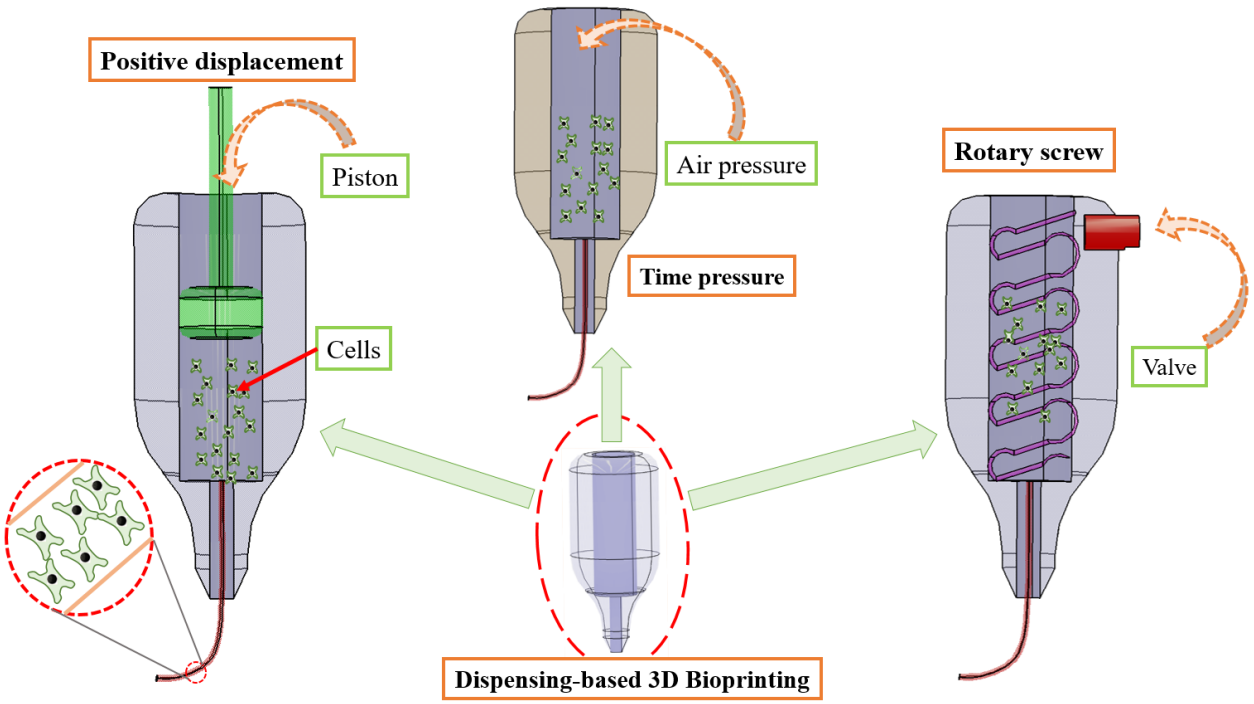

Figure 2. Different types of dispensing-based bioprinting techniques: positive displacement, time pressure, and rotary screw approaches

Dispensing-based bioprinting has been widely used to fabricate cell-laden hydrogels. Biocompatible hydrogel materials mimic the properties of soft tissue, making them excellent materials for cell encapsulation (England et al., 2016). Although hydrogels provide an appropriate environment for cells due to their high water content, they have poor mechanical properties. Thus, hydrogels at higher concentrations have been used to improve printing fidelity but this results in insufficient in-growth of new tissue (Augst et al., 2006). Some hydrogels, such as alginate, do not have attractive biological features and should be modified to be more functional (Shim et al., 2012). On the other hand, other components, such as synthetic polymers, can provide the required mechanical properties but, in the majority of cases, are not biologically compatible (Izadifar et al., 2016). Thus, researchers have combined synthetic/natural hydrogel polymers with the assistance of crosslinkers to improve the mechanical stability of cell-laden hydrogels. Otherwise, the hydrogels can collapse during the printing process due to lack of support (Jung et al., 2010; Kawazoe et al., 2010; Schagemann et al., 2010; Tanaka et al., 2010). These structures fabricated by combining two or more biomaterials to achieve synergistic biological and mechanical properties are called hybrid scaffolds. Typically, dispensing-based hybrid scaffolds reported in the

literature take the form of cell-laden hydrogels and stiffer natural/synthetic polymers (Izadifar et al., 2017). These scaffolds have been widely used in TE applications, such as the regeneration of cartilage, mandible, calvarial bone, peripheral nerve, and skeletal muscle (Izadifar et al., 2012; Kang et al., 2016; Rajaram et al., 2012).

This paper aims to review recent developments with respect to the design and fabrication of hybrid scaffolds based on dispensing-based bioprinting. In this regard, imaging techniques, potential biomaterials, physical architecture, and mechanical properties of hybrid scaffolds are discussed. The importance of vessel-like hollow channels/vascular networks and cell viability, as current challenges in TE, is then highlighted. Finally, the current limitations of 3D bioprinting and future directions for the development of hybrid scaffolds are discussed.

2. Fabrication of hybrid scaffolds for TE

Hybrid scaffolds are bio-fabricated from two or more natural/synthetic polymers in addition to crosslinkers. Figure 3 shows the procedure for the fabrication of hybrid scaffolds. The first step is obtaining imaging data from the patient, followed by generating a CAD model, selecting a biomaterial as well as cell source, and fabricating the hybrid scaffold. To fabricate hybrid scaffolds, a mixture of materials can be printed layer-by-layer or multiple layers of various materials can be combined; in some cases, sacrificial supports are also utilized. Hence, issues including poor mechanical/biological properties of hydrogels can be addressed by combining cell-laden hydrogels with stiffer natural/synthetic polymers in addition to crosslinkers.

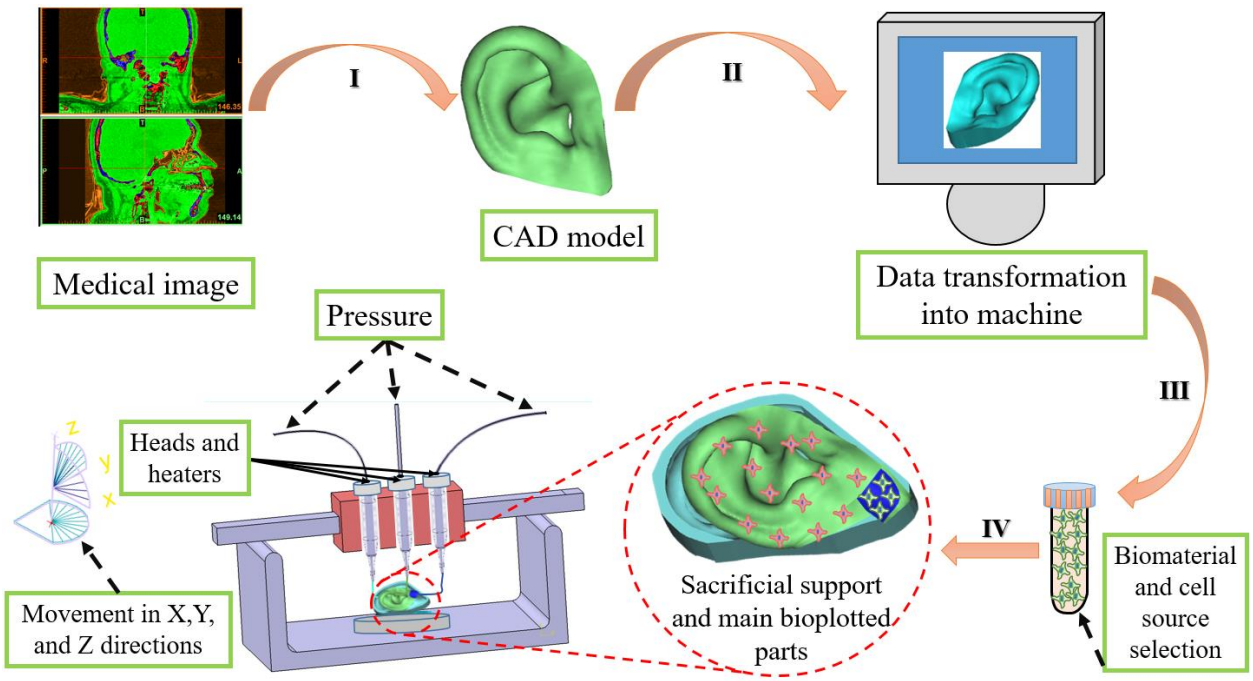

Figure 3. Schematic of the fabrication process of a hybrid ear-shaped scaffold by a dispensing-based 3D bioprinting technique including I) conversion of the medical image to a CAD model, II) transformation of the data to the machine, III) biomaterial and cell source selection, and IV) bioprinting of sacrificial support, auricular cartilage, and fat tissue

Various conventional methods have been used to prepare hybrid scaffolds in which hydrogels were incorporated into the scaffold by perfusion, but inadequate reproducibility and heterogeneous cell positioning limit the application of them (Izadifar et al., 2016). Dispensing-based 3D bioprinting can effectively overcome such limitations. For instance, poly-caprolactone (PCL) and cell-laden alginate hydrogels have been printed using a multi-head tissue/organ building system (MtoBS) (Shim et al., 2012). Using other methods, hybrid scaffolds were fabricated by combining 3D cell printing and electrospinning techniques (Mota et al., 2015; Yeo et al., 2016) or acellular scaffolds using electrospinning and 3D printing together (S. Naghieh et al., 2017; Saman Naghieh et al., 2017).

Depositing biomaterials accurately is the key to mimicking the heterogeneous structures of native tissues. One challenge for both modern and conventional methods used to fabricate hybrid scaffolds is manipulating two or more biomaterials. A common method to manipulate multiple biomaterials is to use multiple dispensers, each depositing a different biomaterial (Khalil and Sun, 2007); this approach has been widely used to create hybrid scaffolds (Schuurman et al., 2011;

Shim et al., 2011). The critical issue of this approach is to control the biomaterials accurately to be deposited as per the CAD model. In other words, the problem associated with this method is the inability to simultaneously and accurately deposit biomaterials/cells. The other possibility for the deposition of multiple biomaterials is to print a mixture of biomaterials, such as a mixture of alginate and gelatin (You et al., 2016a). Simple mixing of various biomaterials/cells and fabricating scaffolds is one of the techniques used to create composite structures and *in situ*-forming hydrogel scaffolds (Macaya and Spector, 2012; Wang et al., 2011). However, accurate control over the deposition of biomaterials/cells is a challenge of this method. To tackle this issue, researchers have leaned towards other techniques such as coaxial nozzle-assisted 3D bioprinting to print biomaterials simultaneously (Gao et al., 2015) and, particularly, to create vessel-like channels, as will be discussed in subsequent sections.

Because hybrid scaffold fabrication requires the handling of multiple biomaterials with different rheological properties, fabrication conditions might need to be rigorously determined and selected. In the dispensing-based technique, continuous and uniform printing of strands is associated with the moving speed of the needle, which is determined by (Tian et al., 2009):

$$V = \frac{4Q}{\pi D^2} \tag{1}$$

where *V*, *Q*, and *D* are the moving speed, flow rate of the dispensed biomaterial, and needle inner diameter, respectively.

Notably, the flow rate of the biomaterial dispensed is a function of operational parameters (e.g., pressure, temperature), the flow behavior of the biomaterial (e.g., viscosity, consistency, flow behavior indexes), and geometric parameters (e.g., needle diameter, length), as given by (M. G. Li et al., 2009):

$$Q = \pi \frac{r_i^3 r_o^3}{4} \left[\frac{3n \tan\theta \left(\Delta P + \frac{2\tau_y}{\tan\theta \ln\frac{r_i}{r_o}}\right)}{2K\left(r_i^{3n} - r_o^{3n}\right)} \right]^{\frac{1}{n}} \tag{2}$$

This equation is for a tapered needle, where *P* is the applied pressure, r_i and r_o are the entrance and exit radius of the needle, respectively, and θ is the angle between needle and deposition surface.

Moreover, τ_y, n, and K are the yield stress, flow index, and consistency index, respectively. Note that n and K are associated with temperature and θ is related to the length of the needle.

Hence, the manipulation of biomaterials used to fabricate hybrid scaffolds is quite challenging. For example, different fabrication parameters have been considered for printing PCL/alginate hybrid scaffolds (Manojlovic et al., 2006; Shim et al., 2012). Generally, a low driving force is needed for hydrogels due to their low viscosity. Furthermore, precise force control is required to print cell-laden hydrogels and arrange cells precisely at high resolution. On the other hand, dispensing materials such as PCL require a higher temperature and driving force. Thus, adequate cooling is required during the printing process of successive layers of hybrid scaffolds to overcome heat-induced cell damage in cell-laden hydrogels.

In addition to the problems associated with manipulating biomaterials in a dispensing-based bioprinting system, liquid polymers are required prior to fabrication. Natural and synthetic polymers require different conditions (e.g., temperature, solvent) to be dissolved and they also need specific conditions (e.g., low temperature, light, crosslinkers, pH) to be crosslinked (Sarker et al., 2015). Therefore, a key challenge in the fabrication of hybrid scaffolds is to manipulate multiple materials with different dissolution and crosslinking or gelation properties. Furthermore, more challenges arise to attach successive printed layers with different biomaterials and when it is required to meet specific fabrication parameters (e.g., extrusion pressure, speed, temperature, type of crosslinker) to achieve printability with geometric precision.

3. Design of hybrid scaffolds for TE

The first step regarding the design of a customized hybrid scaffold could be the creation of a CAD model using medical images (Figure 3). This step plays a decisive role in the biofabrication process with respect to the accuracy of the fabricated scaffold. Biochemical, as well as physical aspects, should be considered in designing tissue scaffolds. Biochemical aspects are associated with the chemical composition and biological properties of the scaffold. Physical design is related to the morphology and mechanical properties of the scaffold. This section highlights imaging techniques and potential biomaterials for the fabrication of hybrid scaffolds. Some fabrication features, morphology, mechanical properties, and how to modulate the mechanical properties of hybrid scaffolds are also discussed.

3.1- Role of imaging techniques and support in the fabrication of custom-made hybrid scaffolds

As illustrated in Figure 3, the fabrication of customized hybrid scaffolds starts with processing medical image obtained from the patient. Imaging data acquisition and conversion into the format recognized by the machine must have sufficient resolution (Naghieh et al., 2016b). Recently, AM and medical imaging techniques, as noninvasive medical imaging modalities, have been used to fabricate customized patient-specific scaffolds (Y. S. Zhang et al., 2017). For example, customized patient-specific implants consisting of autologous cell-laden polymer hydrogels have been reported (Hutmacher et al., 2004; Ricci et al., 2012). To this end, defects of the patient can be scanned using medical imaging and the data obtained then converted into a CAD model (Cazon et al., 2014; Fierz et al., 2008). In fact, computed tomography (CT) and magnetic resonance imaging (MRI) have replaced conventional radiographs to give a 3D view of anatomical regions (da Silva Oliveira Brito et al., 2016). The term computer-aided TE is now considered a hot topic and refers to gaining patients' anatomic data by means of CT or MRI imaging (Sun and Lal, 2002). A comprehensive review has recently been published on the importance of imaging data, challenges, and practical steps needed to fabricate a 3D printed model from cardiovascular CT data (Otton et al., 2017).

Figure 4 illustrates the development of complex organ manufacturing over time using imaging techniques. This process starts with cell encapsulation in biodegradable hydrogels to print large 3D scaffolds; in this regard, the study carried out by Nicodemus and Bryant in 2008 is a good example (Nicodemus and Bryant, 2008). Efforts then switched to the fabrication of artificial organs with more than two types of cells (Murphy and Atala, 2014). Currently, great potential has been demonstrated for the fabrication of custom-made hybrid scaffolds with perfused vascular networks using a combination of 3D bioprinting, imaging, and vascularization techniques (Richards et al., 2017).

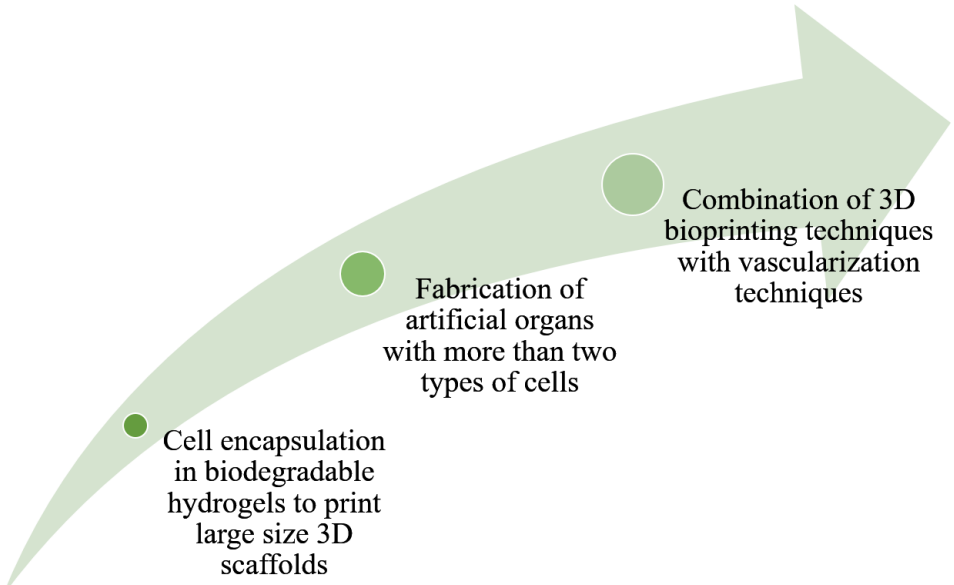

Figure 4. The evolution of complex organ manufacturing based on hybrid scaffolds using medical imaging

Hybrid scaffolds with complex structures are used in various applications, including mandible bone, calvarial bone, ear cartilage, skeletal muscle, and articular cartilage reconstruction (Izadifar et al., 2016; Kang et al., 2016). Biological structures such as the ear (Mannoor et al., 2013) and aortic heart valve (Duan et al., 2013; Hockaday et al., 2012) have been fabricated from polydimethylsiloxane (PDMS) elastomer and alginate hydrogel via syringe-based extrusion. Although combining AM and imaging techniques is a promising method for the fabrication of, for instance, poly (polyetherketoneketone) bone plates (Shah et al., 2014) and PCL tracheal splints (Zopf et al., 2013), it has a critical limitation: in most cases, only soft materials such as hydrogels are printed and the creation of complex structures remains a challenge (Martin et al., 2014; Murphy and Atala, 2014). Complex structures might be defined as large-size structures, such as the ear, that have complex curvatures. More considerations are necessary to fabricate such structures, one of which is having a sacrificial support during their printing.

Fabrication of complex structures, such as the ear, can start from image processing to the fabrication of a custom-made porous scaffold with the assistance of a sacrificial support. Many studies have been conducted in this regard; for instance, Lee et al. used polyethylene glycol (PEG) as a sacrificial support and its removal did not have any detrimental effect on cell viability (J.-S. Lee et al., 2014). Hinton et al. printed complex structures of a 3D model of the heart of a 5-day-

old chick embryo, coronary arterial tree, and human femur by creating a gelatin slurry support bath to support the main structure during printing (Hinton et al., 2015). In another study, Pluronic F-127 hydrogel was used as a support just before crosslinking of the hydrogel (Kang et al., 2016). Lee et al. reported the regeneration of both auricular cartilage and fat tissue after printing a PCL and cell-laden hydrogel; they used PEG as a sacrificial layer to support the complex structure of the ear (J.-S. Lee et al., 2014). Another study reported a supramolecular assembly (guest-host system) for the development of bioinks and support hydrogels, such that filaments were deposited in the support hydrogel (Highley et al., 2015). Using a slurry of gelatin microparticles is another method to support complex 3D structures during printing (Hinton et al., 2015). In a similar study, a soft granular gel was used as a support medium and alginate droplets were dispensed into a bath of $CaCl_2$ as a crosslinker (Bhattacharjee et al., 2015; Christensen et al., 2015). Additionally, some researchers used a submerged-in-crosslinker approach to crosslink the hydrogel just after printing to create hybrid scaffolds with cell-laden hydrogels (Gao et al., 2015; You et al., 2016b).

Sacrificial support is required for the fabrication of complex structures, as depicted for the ear in Figure 5. Supports are quiet useful assets to tolerate the weight of material during the printing process of a structure and specifically for situations, that material cannot be printed without support. The process starts with the generation of a CAD model using imaging data and progresses to the fabrication of a porous scaffold. The ear has a complex shape and composition and is a good candidate to illustrate the complexity of printing such structures. Notably, the ear has both auricular cartilage and fat tissue and, thus, bioprinting of the ear is also a good example of the fabrication of hybrid scaffolds using various biomaterials. Figure 5.a shows the 3D model of the ear created using imaging data. This 3D model is then converted to an STL file and, after ensuring its accuracy, different parts, support, and the final porous structure can be designed (Figure 5.b). It is worth mentioning that the regeneration of ear tissue with traditional techniques is difficult.

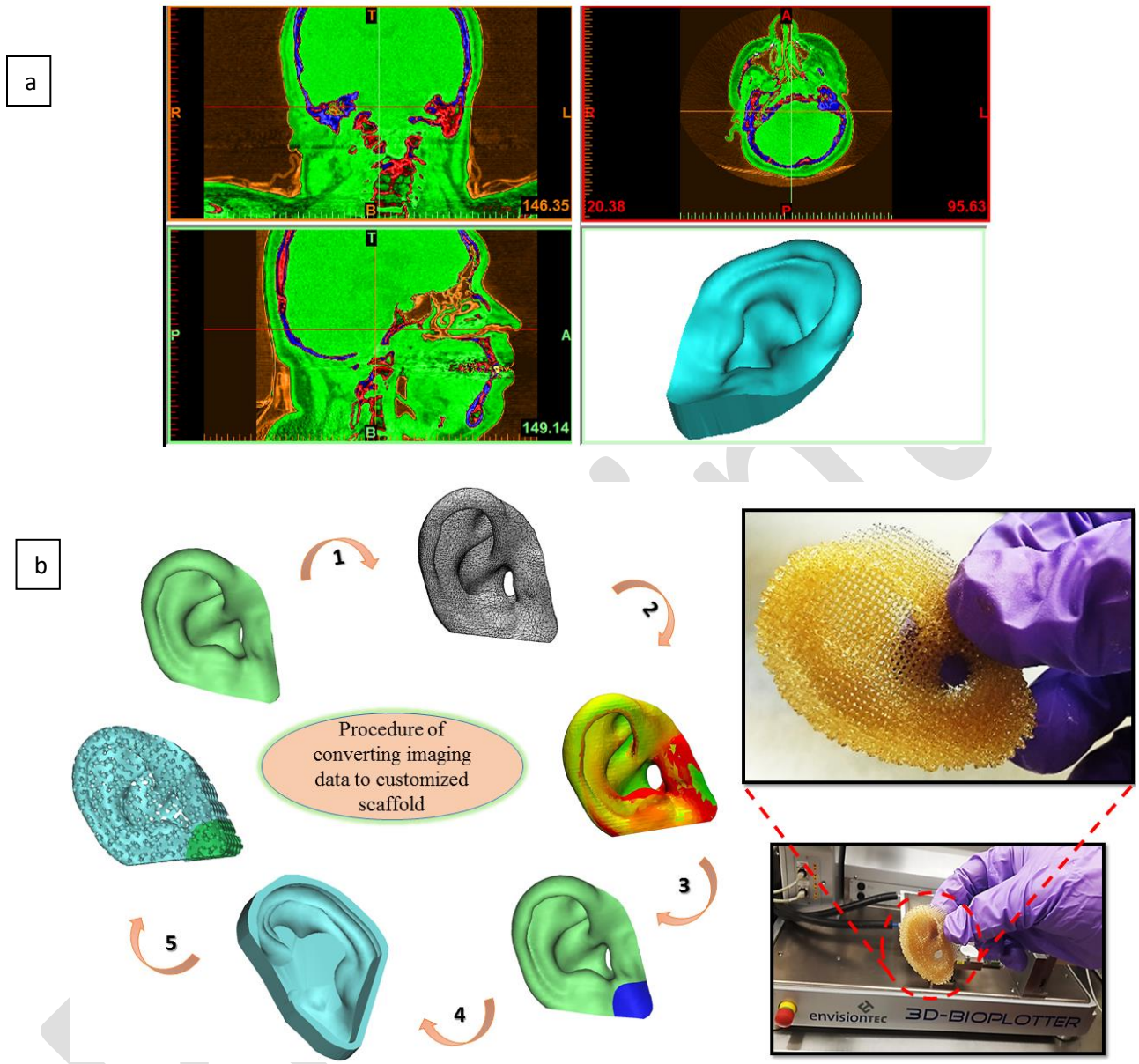

Figure 5. 3D biprinting of complex structures via sacrificial support for ear regeneration: a) obtaining CAD model from imaging data, b) left picture: 1- converting CAD model to STL file, 2- investigation of the accuracy of STL file, 3- defining desired parts for bioprinintg with different cells, 4- creation of the CAD model of sacrificial support based on main CAD model, 5- fabrication of porous scaffold via bioprinter, right picture: a representative sample of ear fabricated by a 3D-Bioplotter (CAD model is available at https://www.thingiverse.com/thing:304657 (Addamay123, 2017))

3.2- Potential biomaterials used in the fabrication of hybrid scaffolds

Biomaterials should act as a mechanical support and provide biological requirements for targeted cells selected based on application. Hydrogels, such as alginate, are good substrates for

the incorporation of cells but do have not appropriate mechanical stability. To address this issue, hybrid scaffolds, including hydrogels and other natural/synthetic components, are used. From the biological point of view, many efforts have been made to fabricate functionalized scaffolds. Moreover, extracellular mimetic hydrogels are outstanding examples used in various biomedical applications that provide an artificial extracellular microenvironment resembling both the mechanical and biological features of extracellular matrix (ECM). Such structures have been applied to cartilage, bone, tendon, and intervertebral disc regeneration (Lv et al., 2013).

In addition, the selected biomaterials should be biocompatible to support cell activities such as proliferation, migration, etc. (Ferris et al., 2013). Moreover, they should have a suitable degradation rate and non-toxic byproducts to degrade just after tissue regeneration and replacement of ECM proteins. A degradation rate that is too fast/slow results in issues such as lack of stability of the biomaterial (Ning and Chen, 2017). Moreover, the selected biomaterials should be printable with suitable fluidic viscosity. In this regard, some biomaterials have good printability (Fedorovich et al., 2008); for those with poor printability, methods such as the use of sacrificial materials can be utilized. When using hydrogels in a dispensing-based system, good crosslinkers should be used to prevent any collapse during the printing process (Murphy and Atala, 2014). Hence, many factors including printability, degradation rate, mechanical stability, biological requirements, etc. should be taken into account during biomaterial selection,

Both synthetic and natural polymers have been widely used in TE applications. Some synthetic polymers used in scaffold fabrication cannot provide an appropriate environment for cell attachment because they are hydrophobic and do not have cell attachment sites. In contrast, hydrogels are good candidates for cell encapsulation and 3D bioprinting but have poor mechanical properties. Hence, the combination of synthetic biomaterials (or other components) and hydrogels creates potential constructs for 3D biofabrication (Kundu et al., 2015a).

To overcome the poor mechanical properties of cell-laden hydrogels, several efforts have been made to combine hydrogels and other synthetic/natural polymers using a dispensing-based technique to support cell-laden hydrogels (Kim et al., 2015; Yeo et al., 2016). In this regard, Kang et al. reported the fabrication of hybrid scaffolds by combining cells with gelatin, fibrinogen, hyaluronic acid (HA), and glycerol mixed into Dulbecco's Modifies Eagle Medium (DMEM) (Kang et al., 2016). In a similar study, PCL improved the mechanical stability of cell-impregnated

alginate for cartilage tissue regeneration (Izadifar et al., 2016). In addition to mechanical properties, shear-thinning materials are generally desired candidates for 3D dispensing-based bioprinting due to the rapid decrease of viscosity of the material after extrusion from the nozzle (Shim et al., 2012).

Hydrogels can be functionalized to improve their biological properties. For instance, one polysaccharide-based hydrogel widely used in dispensing-based bioprinting is alginate, which has good biocompatibility, low toxicity, and high printability (Ahn et al., 2015; Andersen et al., 2015; Perez et al., 2013). This biomaterial has been successfully used to incorporate pancreatic islet cells, fibroblasts, myoblasts, and chondrocytes (Bohari et al., 2011). In spite of many attractive features, a lack of cell binding sites limits the application of sodium alginate; for instance, Shim et al. reported that alginate (derived from brown seaweed) might not promote cellular activities because it has no bioactive proteins (Shim et al., 2012). In this regard, many efforts have been made to functionalize alginate. For example, carbodiimmide chemistry is useful for forming covalent bonds between various peptides and the alginate molecule. Such peptides can significantly enhance the functionality of cell-laden alginate for neurite outgrowth (Bettinger et al., 2006). In this regard, the lack of adhesion sites on alginate has led researchers to functionalize this polymer by adding peptides, fibronectin, laminin, fibronectin, collagen, gelatin, etc. (Dhoot et al., 2004; Matyash et al., 2012; Novikova et al., 2006). Another option for functionalizing hydrogels is the addition of immobilized growth factors, e.g., to functionalize chitosan hydrogel for the differentiation of neural stem cells (Lv et al., 2013).

Another point to take into account is that selected biomaterials utilized in the fabrication of hybrid scaffolds should have a proper degradation rate. For example, hybrid scaffolds have been fabricated using cell-laden alginate hydrogel and PCL (Izadifar et al., 2016); however, all of the pores were filled with gel and eliminated channels available for nutrient perfusion. Thus, the rate of degradation should be appropriate so that the scaffold degrades and provides some channels for perfusion. The issue of lack of nutrients, specifically for the inner parts of the scaffolds, has been extensively discussed elsewhere (Izadifar, 2013). To address this issue, radio frequency heating has been used to accelerate the biodegradation of scaffolds and create a pathway for nutrient perfusion (Izadifar and Chen, 2013). A recent review discusses the challenge of how to match the degradation rate of scaffolds with the growth of native tissue (Yang et al., 2017). Other researchers

have tried to fabricate hybrid scaffolds with pores intentionally left empty for oxygen and nutrient transport and as an example refer to (Shim et al., 2012).

Overall, the biomaterials selected for hybrid scaffolds should satisfy both mechanical and biological requirements. Table 2 lists the potential biomaterials that can be utilized in the fabrication of hybrid scaffolds as well as dispensing-based printing machines used in the biofabrication of hybrid scaffolds.

Table 2. Potential biomaterials and printing parameters used in the biofabrication of hybrid scaffolds

Materials	Application	Description	Dispensing-based printing machines	Ref
PCL and alginate	Osteochondral tissue regeneration	PCL (molecular weight = 70000–90000 Da), 4% w/v alginate	MtoBS	(Shim et al., 2012)
PCL and alginate	Generation of organized living grafts with improved mechanical stability	PCL (molecular weight = 70000–90000 Da), 2% w/v medium viscosity sodium alginate	BioScaffolder dispensing: multi-arm dispensing-based bio-printing system	(Schuurman et al., 2011)
Nanofibrillated cellulose (NFC), PCL, and alginate	Auricular cartilage regeneration	2% (w/w) of plant-derived NFC, PCL Capa 6500, 0.5% (w/w) sodium alginate	3D Discovery® instrument	(Martínez Ávila et al., 2016)
PCL, Pluronic F-127, hydrogel: gelatin, fibrinogen, hyaluronic acid (HA) and glycerol	Bone, cartilage, skeletal muscle	PCL (molecular weight =43000~50000 Da), gelatin (35~45 mg/mL), fibrinogen (20–30 mg/mL), HA (3 mg/mL), and glycerol (10% v/v), 33% w/v Pluronic F-127 added to a 10% v/v glycerol solution.	Integrated tissue and organ printing (ITOP)	(Kang et al., 2016)
PCL, PEG, alginate	Ear regeneration	PCL (molecular weight =45000-60000 Da), PEG (molecular weight = 20000 Da), 4% w/v alginate	MtoBS	(J.-S. Lee et al., 2014)

Fibrinogen, collagen type I, and Matrigel	3D printed bifurcated tubes	-	MakerBot Replicator printer	(Hinton et al., 2015)
Cell-laden sodium alginate (Na-Alg) and $CaCl_2$	Micro-channels for nutrients delivery	2-5% (w/v) Na-Alg solution 2-5% (w/v) $CaCl_2$	Coaxial nozzle-assisted 3D bioprinting system	(Gao et al., 2015)
Alginate, HA	Peripheral nerve regeneration	Alginate and HA (2.5 % w/v alginate and 0.25 % w/v HA)	3D-Bioplotter™ system, EnvisionTEC	(Rajaram et al., 2014)
PCL and alginate	Cartilage TE	PCL (molecular weight =48000-90000 Da); Alginate: 2 and 2.5% medium viscosity alginate	3D-Bioplotter™ system, EnvisionTEC	(Izadifar et al., 2016)
Collagen hydrogel precursor, gelatin, fibrinogen, thrombin	Vascular Network System	10% (w/v) gelatin, collagen hydrogel precursor (rat tail, type I), fibrinogen (10 mg/mL), thrombin (3U/mL)	A developed bio-printing platform	(V. K. Lee et al., 2014b)
PCL and alginate	Cartilage TE	PCL (molecular weight =70000-90000 Da), 4 and 6% alginate	Multihead deposition system (MHDS)	(Kundu et al., 2015a)
Collagen, gelatin	Fluidic channels	Collagen hydrogel precursor (rat tail, type I), 7% (w/v) gelatin	Bio-printer system	(W. Lee et al., 2010)
PCL, PEG, alginate/ atelocollagen/ decellularized ECM	Heterogeneous tissue regeneration	PCL (molecular weight =70000-90000 Da), PEG (molecular weight = 20000 Da),	MtoBS	(Pati et al., 2013)
Oxidized alginate, gelatin	Processability of the oxidized alginate-gelatin hydrogel in bioplotting applications	2% (w/v) sodium alginate (molecular weight of 100000–200000 g/mol), gelatin (type A)	Three axes moveable bioplotter (type BioScaffolder 2.1)	(Zehnder et al., 2015)
PCL and alginate	Soft and hard tissue regeneration	PCL (molecular weight =60000-80000 Da), 3.5 wt% alginate (low viscosity, high G-content non-medical grade LF10/60)	Dispensing system	(Lee et al., 2013)

3.3- Physical architecture of hybrid scaffolds

The morphology of a scaffold is defined by the geometry, distribution, and interconnectivity of pores, which are considered to be key parameters for 3D scaffold fabrication (Izadifar et al., 2012). Due to the dependency of the mechanical properties into on the geometrical characteristics of the scaffold, here we emphasize the physical architecture; and in the next subsection, mechanical properties are discussed separately. In particular, in a porous scaffold, the macropores support cell migration whereas micropores promote cell–cell interactions and mass transport. Moreover, larger pores facilitate ECM extension and small pores enhance cell proliferation (El-Ayoubi et al., 2011; Lien et al., 2009). A recent review emphasizes the physical architecture of scaffolds in tissue regeneration (Hinton et al., 2017). To facilitate cell–cell interactions, mass transfer within the designed hybrid scaffold should be facilitated by sufficient mechanical stability in a porous structure with interconnected pores. Furthermore, interconnected pores ensure homogeneous cell seeding and better nutrient diffusion (El-Ayoubi et al., 2011, 2008; Klein et al., 2009).

In general, hybrid scaffolds require a porous structure with interconnected pores due to the dependency of initial cell–carrier substance impregnation, cell–cell interactions, mass transfer of nutrients, and tissue growth to this factor. Therefore, balance among various design parameters must be achieved as strand thickness, pore geometry, and porosity significantly affect the mechanical and biological performance of the printed scaffold. In this regard, You et al. showed that the mechanical properties of hydrogel scaffolds can be modulated by altering internal structure parameters, including strand orientation and spacing, to manipulate the physical architecture of the scaffold (You et al., 2016a). In another study scaffolds with high porosity facilitate cell attachment were reported (Spiteri et al., 2006). In a dispensing-based system, the main factors affecting the morphology of hybrid scaffolds are operating temperature, pressure, nozzle speed, and nozzle diameter. One of the advantages of developing hybrid scaffolds is that hydrogels cannot provide 3D constructs with pre-defined internal architectures; only a few reports are available in this regard (Cohen et al., 2006; Guillotin et al., 2010). Generally, changing the physical features of scaffolds (e.g., pore size, strand width) results in changes to mechanical properties, to be discussed in the next section.

Table 3 summarizes the physical and mechanical properties of bioprinted hybrid scaffolds. The diameter of the dispensed strands depends on the pressure, temperature, nozzle size, and nozzle speed. PCL strands with various diameters (50 to 275 µm) have been printed by adjusting the aforementioned fabrication variables (Shim et al., 2012). In particular, changing these variables regulates the flow rate of the material dispensed from the needle/nozzle. In this regard, numerous models have been developed to predict the flow rate of the dispensed biomaterial to fabricate scaffolds with expected pore size and strand width (Chen et al., 2008; Sarker and Chen, 2017).

Table 3. Physical architecture and mechanical properties of hybrid scaffolds

Materials	**Strand width (µm)**	**Pore size (µm)**	**Mechanical properties (KPa)**	**Description**	**Reference**
PCL and alginate	50-275	50-600	-	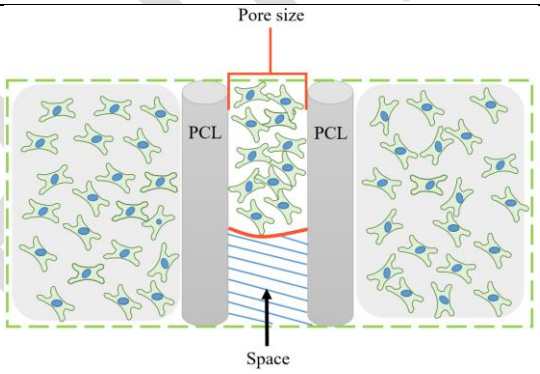	(Shim et al., 2012)
PCL and alginate	-	2000	Young's modulus near 600	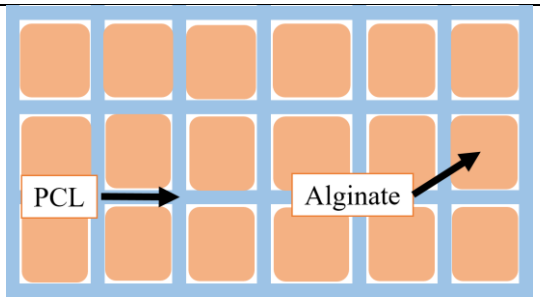	(Schuurman et al., 2011)
PCL, NFC (cellulose), alginate	Refer to picture	Theoretical porosity of 50%	-	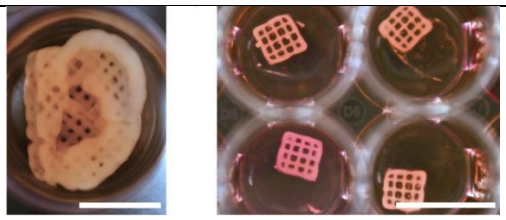 Scale bar = 1 mm, with permission from the respective publisher	(Martínez Ávila et al., 2016)

PCL, Pluronic F-127, hydrogel: gelatin, fibrinogen, HA, and glycerol	~ 370	~ 750	Three-point bending test of the 3D bioprinted ear constructs for 1 mm extension: percentage of loading cycle 49.22 ± 12.54 (pre-implantation), 29.58 ± 3.45 (after one month)	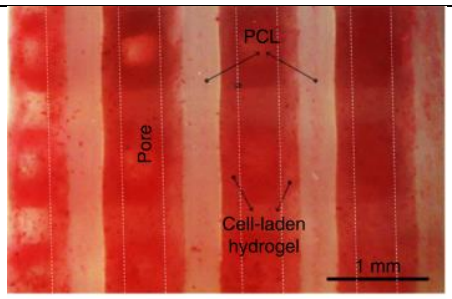 With permission from the respective publisher	(Kang et al., 2016)
PCL, PEG, alginate	200	600	Tensile modulus 14000–16000	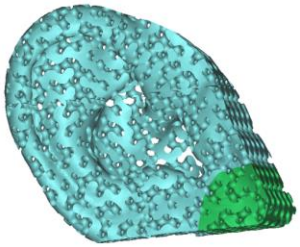	(J.-S. Lee et al., 2014)
Cell-laden sodium alginate (Na-Alg) and $CaCl_2$	Outer diameter of hollow tube: 1192	Inner diameter of hollow tube: 892	Ultimate tensile strength of 3D structure based on fusion of adjacent hollow filaments: 46 (2% alginate), 77 (3% alginate), 116 (4% alginate)	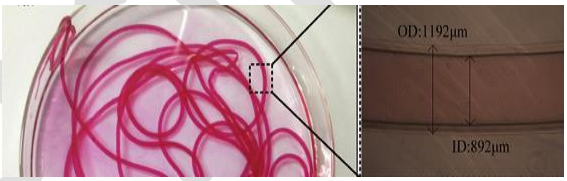 With permission from the respective publisher	(Gao et al., 2015)
PCL and alginate	~ 400	~ 650	-	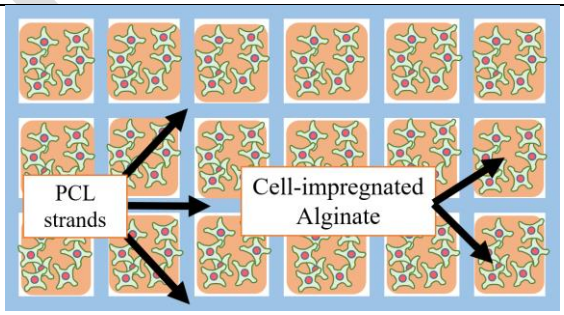	(Izadifar et al., 2016)
PCL and alginate	200 ± 20	400 ± 20	-	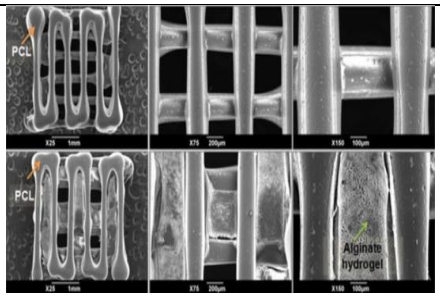 With permission from the respective publisher	(Kundu et al., 2015b)

PCL and alginate (only PCL was printed)	200-400	1000-2000	PCL compressive modulus: 6630-56460 PCL tensile modulus: 6030-46040 Compressive modulus of alginate was considered negligible	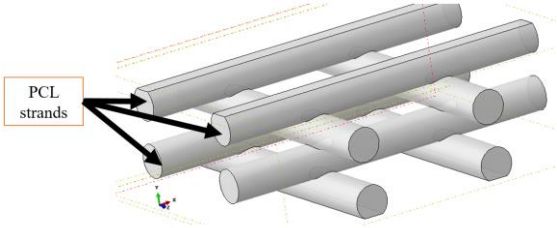	(Olubamiji et al., 2016)
PCL and alginate	Alginate: 466 ± 63, PCL: 437 ± 11	88 ± 47	Tensile modulus: 15400 and 8300	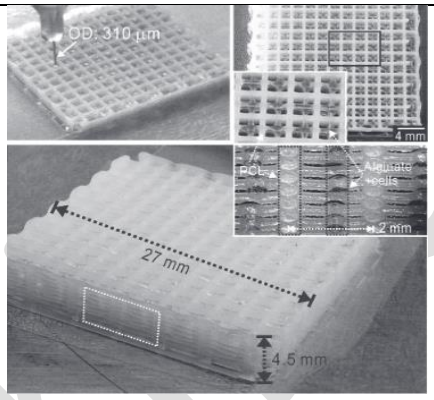 With permission from the respective publisher	(Lee et al., 2013)

3.4- Mechanical properties: hybrid scaffolds with tailorable mechanical properties

As discussed above, stiffer materials are generally used to improve the mechanical properties of hydrogel biomaterials. Many studies cite the poor mechanical properties of hydrogels as evidence to justify the fabrication of hybrid scaffolds (Hölzl et al., 2016; Izadifar et al., 2016; Olubamiji et al., 2016; Shim et al., 2012). Because a hybrid scaffold might be a combination of a soft material and a stiff material, mimicking the mechanical properties of native tissue is quite challenging. Successful tissue regeneration largely depends on the mechanical properties of fabricated scaffold resembling native tissues. Different studies have made efforts to tailor the mechanical properties of scaffolds by exploring appropriate biomaterial and scaffold geometry (Moroni et al., 2005; Woodfield et al., 2004). In addition to experimental studies, some efforts have been made to predict the mechanical properties of scaffolds using numerical investigation. Numerical studies have been carried out to reduce the number of experiments to evaluate scaffolds using finite element models (Karamooz Ravari et al., 2015; Naghieh et al., 2016a; Ravari and Kadkhodaei, 2013). In this regard, more studies should be done to develop models that can predict the mechanical behavior of scaffolds considering the effects of geometric features. Inconsistency

between the mechanical properties of scaffolds and native tissues provokes a stress-shielding phenomenon and, thus, inhibits ECM secretion by cells (Olubamiji et al., 2016). According to the literature, various mechanical properties are desired with respect to the application of hybrid scaffolds; Table 3 presents mechanical properties of some hybrid scaffolds utilized in different applications.

Hybrid scaffolds with tailorable mechanical stiffness (provided by thermoplastic polymers) have been printed together with cells (Schuurman et al., 2011). In particular, hybrid scaffolds composed of an acellular and soft matrix were fabricated to mimic specific native tissues and achieve the desired biomechanical and biological function (Eyrich et al., 2007; Hayami et al., 2010; McMahon et al., 2011; Nerurkar et al., 2010). Likewise, the spacing, orientation, and thickness of the fibers of hybrid scaffolds have been modified to improve mechanical properties in order to for use in intervertebral disks, cartilage, bone, and ligaments, and even in large blood vessels (Gloria et al., 2007; Holloway et al., 2010; Moroni et al., 2006). Cardiac implants with modulated mechanical properties have been reported using hydrogel bioprinting with various patterns (Izadifar et al., 2017). With respect to tailorable mechanical properties, more investigations are needed as this area is under-explored. Further, modulating the molecular weight of PCL and scaffold geometry has been attempted to fabricate hybrid constructs with similar mechanical properties to cartilage tissue (Olubamiji et al., 2016). Notably, conventional methods are unable to provide scaffolds with tailorable mechanical properties due to random pore size and distribution, uncontrollable porosity, and poor pore interconnectivity (Correlo et al., 2009; Lebourg et al., 2008; Lin et al., 2003; Moroni et al., 2006).

Beyond the general goal of creating 3D scaffolds with mechanical properties similar to native tissues, the mechanical properties of scaffolds can affect vascularization. For example, cells respond to the mechanical properties of implanted scaffolds (Wen et al., 2014). Santos et al. showed that human umbilical vein endothelial cells (HUVECs) grown on collagen-coated low and high stiff polyacrylamide hydrogels showed different functional expression (Santos et al., 2015). Another study demonstrated that endothelial cells respond differently to angiogenic growth factors according to the mechanical properties of the scaffold (Shamloo and Heilshorn, 2010). Consequently, a vascular organization can be controlled via scaffolds by modulating mechanical properties; this effect can be useful to better control the creation of vascular networks.

4. Cell viability and scaffold activation in large hybrid constructs: the role of vessel-like hollow channels/vascular networks

Creating vascular networks with perfusion capability within 3D thick scaffolds is one of the most critical challenges in the fabrication of large scaffolds for maintaining the viability of cells (Mironov et al., 2009); this important issue is the subject of a recent review (Kim et al., 2016). The creation of large hybrid scaffolds is no exception as large hybrid structures require appropriate vessel-like hollow channels/vascular networks to support cell viability throughout the 3D construct regardless of application. The creation of vessel-like hollow channels/vascular networks is not only important for vascularization using endothelial cells (ECs) but also vital for other applications using various types of cells. Vessel-like hollow channels/vascular networks play a major role in maintaining cell viability by facilitating adequate transport of oxygen and nutrients to the cells (Bae et al., 2012; Nomi et al., 2002; Zhang and Khademhosseini, 2015). The goal of the creation of hollow channels within scaffolds is to improve the cell viability in bioprinted scaffolds compared to those created with traditional scaffold-based TE techniques. This is considered a promising approach allowing the fabrication of complicated tissues for major internal organs, handling and positioning of multiple cell types, and integrating a vascular network in 3D tissue structures (Mironov et al., 2008; Nakamura et al., 2010). As an example of the importance of a hollow channel/vascular network, the lack of a network within a PCL/alginate hybrid scaffold reduced cell viability after just three days of culture (Schuurman et al., 2011). To address this issue, several attempts have been made to facilitate media transport within controlled scaffold geometry but failed due to the absence of integrated vascular networks (Yu et al., 2014). In this section, methods used to create vessel-like hollow channels/vascular networks and how to activate scaffolds for vascularization are discussed; the effect of printing parameters on cell viability is then summarized.

Notably, some approaches, such as chemical modification of biomaterials, optimization of pore sizes to facilitate blood vessel ingrowth, incorporation of angiogenic factors (Zhu et al., 2016), and prevascularization of the scaffold in a bioreactor can enhance the formation of vasculature within a hybrid scaffold. Generally, microfabrication (e.g., photo patterning, micro-molding) and 3D bioprinting techniques are suitable for creating vascular networks (Rouwkema and Khademhosseini, 2016). Embedded microfluidic networks can improve perfusion in thick

scaffolds but, in the majority of cases, microfluidic fabrication methods require various processes and, thus, direct fabrication of a vascular network is not possible (Andersson and Van Den Berg, 2004). Generation of a micro-pattern requires the knowledge of microfluidics to regulate the microenvironment (gas transfer, shear stress on cells, etc.) in cell culture. One example in this regard is using stacked multiple layers of poly (glycerol sebacate) embedded with microfluidic networks to promote the formation of a complex vascular network within a 3D scaffold (Bettinger et al., 2006). Moreover, sacrificial filaments (carbohydrate glass) incorporated within a 3D scaffold are useful for generating a vascular pattern, but this approach is not free from the complexities introduced by ECs seeding and the need to remove the sacrificial material. With respect to vascular networks, Huang et al. reported the fabrication of 3D zigzag cellular tubes according to the fusion of sodium alginate droplets via inkjet printing. However, this method requires the precise deposition of sodium alginate droplets and long printing times (C. Xu et al., 2012). Another technique uses matrix-assisted pulsed laser evaporation; however, this method requires highly viscous materials and thus results in poor cell survival (Yan et al., 2012). Although seeding and encapsulation methods have been used to incorporate ECs within scaffolds, they can only form randomly organized vessels with poor interconnectivity.

Similar to the fabrication of complex structures with the assistance of sacrificial biomaterials as mentioned in the previous sections, several studies have used sacrificial techniques for vascular architecture fabrication. A recent review focuses on the utilization of sacrificial bioink materials for bioprinting of vascular tissue scaffolds (Datta et al., 2017). However, ECs cannot be encapsulated during the fabrication of vascular channels in these methods (Gao et al., 2015; W. Lee et al., 2010; Wu et al., 2010). For instance, carbohydrate glass scaffolds were bioprinted but the sacrificial materials did not quickly dissolve after immersion in the culture medium (Miller et al., 2012). In other studies, a perfused vascular channel was prepared in which a gelatin-based sacrificial filament was embedded into a collagen scaffold (V. K. Lee et al., 2014a), and porous PCL bone grafts were vascularized through the post-seeding of human adipose-derived stem cells with a heterogeneous distribution (Temple et al., 2014). Figure 6 illustrates the various techniques utilized in the creation of vascular networks within hybrid scaffolds. These techniques use a hydrogel reservoir to print in a bath of the hydrogel as a support. Second, coaxial nozzle printing can be utilized to create hollow channels using simultaneous crosslinking of the hydrogel. This technique is also known as core-shell printing and is a good candidate for the creation of hollow

channels that can be used for drug delivery (Perez and Kim, 2015) or vessel-like channels as reported by many researchers (Datta et al., 2017; Jia et al., 2016; Z. Zhang et al., 2017). Third, sacrificial materials act as a support that can be removed after chemically crosslinking of the main matrix. Using this method, Norotte et al. reported the creation of hollow channels of multicellular pig smooth muscle cells with the assistance of agarose cylinders as a sacrificial biomaterial (Norotte et al., 2009).

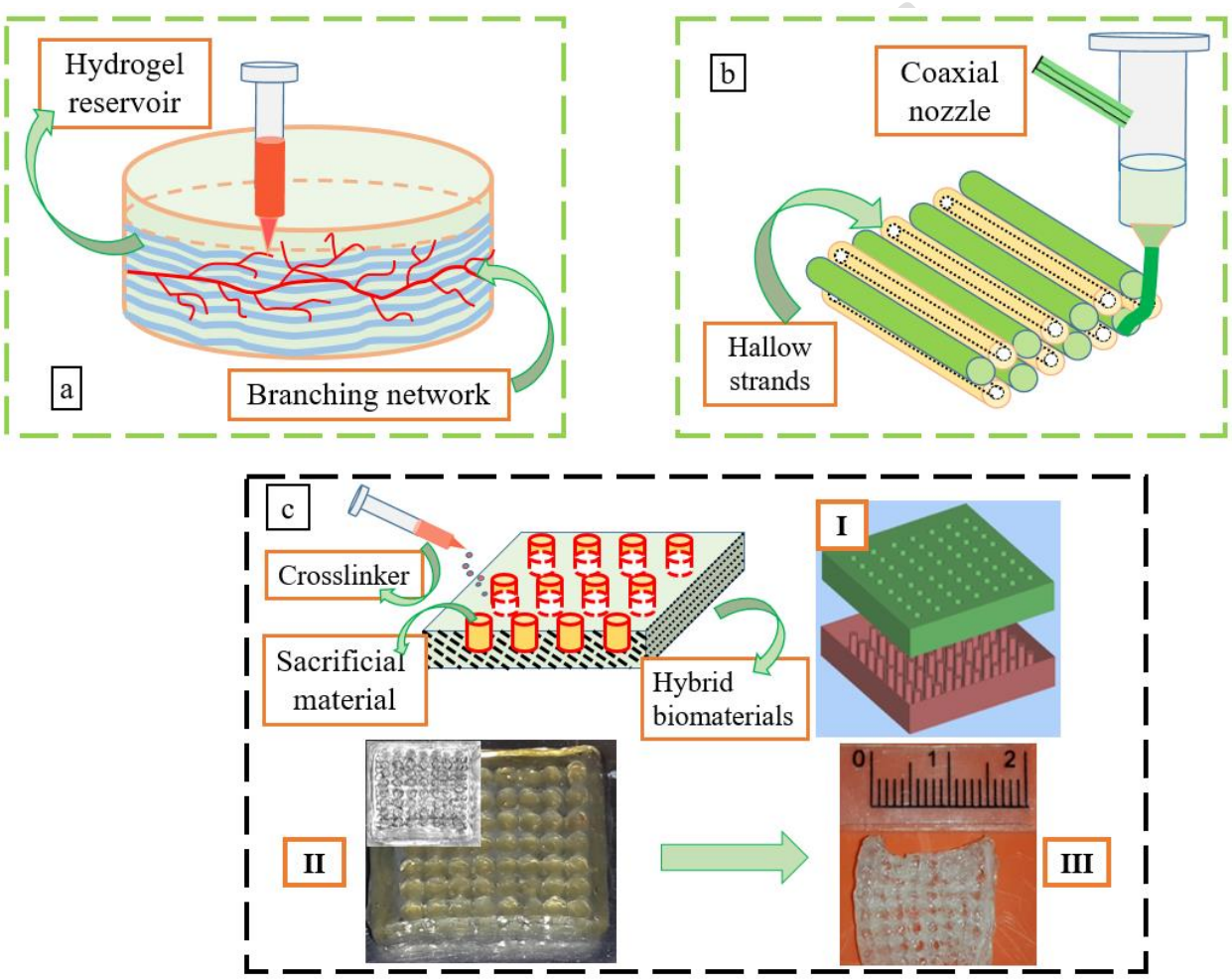

Figure 6. Printing of vascular networks within hybrid scaffolds using: a) hydrogel reservoir, b) coaxial nozzle, c) sacrificial material: I) CAD models of main (hybrid biomaterials) and sacrificial parts, II) final scaffold before removing sacrificial material (inset is the top view during fabrication), III) final hybrid scaffold after removal of the sacrificial material

Moreover, hybrid scaffolds can be created from a 3D construct fabricated from functional biomaterials. Bioactive molecules such as cell-adhesion peptides, responsive moieties, and growth

factors incorporated into 3D scaffold can enhance biological function and vascularization (Hoffman, 2012; Martino et al., 2013; Purcell et al., 2014). Sequential release of various angiogenic factors (such as vascular endothelial growth factors, basic fibroblast growth factor, and platelet-derived growth factor) from 3D scaffolds stimulates vasculature formation and therefore has frequently been explored (Y. S. Zhang et al., 2017). Assembling multiple autologous cells, growth factors, and bioactive agents, mimicking the native tissue, is quite challenging; however, a 3D bioprinter with multiple nozzles can efficiently overcome this difficulty. A strategy to deploy stem cells and growth factors together in large constructs to form vascular networks through the proliferation and differentiation of stem cells has been successful (Wang et al., 2016). Hybrid scaffolds including tricalcium phosphate, PCL, and cells supported large blood vessel formation in calvarial bone reconstruction, while the control group promoted limited vascularization in the periphery of the implant (Kang et al., 2016). The difficulty associated with thick tissue vascularization is forming an integrated vascular network within the 3D scaffold to allow the delivery of growth factors, oxygen, and other nutrients, and therefore this issue has been studied intensively (Chrobak et al., 2006; Ozbolat and Yin Yu, 2013).

The importance of using vessel-like hollow channels/vascular networks is to ensure cell viability. However, printing parameters also affect cell viability. Needle geometry and pneumatic pressure can affect cell viability in the 3D vascular pattern fabricated by a dispensing-based system. Using this method, many factors should be considered regarding cell viability and printing cell-laden hydrogels. For instance, conical needles are superior to cylindrical needles with respect to shear-induced cell damage, and therefore tapered needles are recommended (Izadifar et al., 2016). Additionally, highly viscous hydrogels offer better printability but cause cell damage in the printing process due to higher dispensing pressure (Nair et al., 2009). Some of the printing parameters and conditions used in the biofabrication of hybrid scaffolds for different TE applications are summarized in Table 4. A lower pneumatic pressure is recommended for cell-laden hydrogel printing to reduce the shear stress, which is one of the main factors influencing cell viability. Another factor is needle diameter, where smaller needle diameters result in more cell damage. Applied temperature and needle length are other paramount factors (Li et al., 2010).

Table 4. Printing parameters and reported cell viability for different kinds of cells

Materials	Nozzle speed/feed rate (mm/min)	Needle diameter (μm)/gauge size	Pressure (KPa)	Temperature (°C)	Crosslinking of hydrogel (mM)	Cell types	Cell viability	Description	Reference
PCL and alginate	Scan speed of the head PCL: 100 Alginate: 250	PCL: 200 and 150	PCL: 400 Alginate: piston-based system with a plunger speed of 1.2 mm/min	PCL: 80 Alginate: 20	$CaCl_2$: 100 and NaCl: 145	Chondrocytes isolated from human nasal septum cartilage and osteoblasts	Chondrocytes (~93.9%) and osteoblasts (~95.6%)	Cell viability for at least 7 days; chondrocytes retained their viability without remarkable proliferation after 7 days	(Shim et al., 2012)
PCL and alginate	PCL: feed rate of 176 Alginate: deposition speed of 100	PCL: 23G Alginate: 210	PCL: 500 Alginate: piston-based system with a plunger speed of 1.5 mm/min	PCL: 160 Alginate: room temperature	$CaCl_2$: 102	C20A4 cells	More than 60%	Only first day	(Schuurman et al., 2011)
Nanofibrillated cellulose (NFC), PCL, and alginate	Feed rate PCL: 1200 NFC-Alginate: 300	PCL: 330 NFC-Alginate: 150	PCL: 250 NFC-Alginate: 40	PCL: 90 NFC-Alginate: 23	$CaCl_2$: 100	Human nasal chondrocytes (hNC)	~70.9%	Throughout 28 days	(Martínez Ávila et al., 2016)
PCL, Pluronic F-127, hydrogel: gelatin, fibrinogen, HA, and glycerol	-	PCL: 250 Pluronic F127: 250 Cell-laden hydrogel: 300	PCL: 800 Pluronic F127: 200-300 Cell-laden hydrogel: 50~80	PCL: 92.5 Others: 18	Thrombin solution (20 UI/mL)	3T3 fibroblasts and Human AFSCs, rabbit ear chondrocyte, mouse C2C12 myoblasts	3T3 fibroblasts ≥ 95% ~91% for AFSCs and chondrocyte and ~97% for myoblasts C2C12 myoblasts	3T3 fibroblasts: on day 0, maintained through days 3 and 6 and other cells for long durations	(Kang et al., 2016)
PCL, PEG, alginate	PCL: scan velocity 205 Alginate: piston velocity 0.48	-	PCL: 650 PEG: 300	PCL: 80 PEG: 80	$CaCl_2$: 100	Chondrocytes and adipocytes differentiated from adipose-	~95%	During 7 days	(J.-S. Lee et al., 2014)

				Alginate: room temperature		derived stromal cells			
PCL, PEG, Alginate/ atelocollagen/ decellularized ECM	Scan velocity, PCL: 205 PEG: 310 Alginate: 80 Atelocollagen: 60 dECM: 55	250	PCL: 650 PEG: 300 Piston velocity of alginate, Atelocollagen, and dECM: 0.008, 0.015, and 0.018 mm/s, respectively.	PCL: 80 PEG: 80 Others: room temperature	$CaCl_2$	Human adipose-derived stem cells (hASCs) and human-turbinate-tissue-derived mesenchymal stem cells (hTMSCs)	>95%	-	(Pati et al., 2013)
Fibrinogen, collagen type I, and Matrigel	-	150	-	22	Printing in a gelatin slurry	C2C12 myoblasts	~99.7%	During 7 days	(Hinton et al., 2015)
Cell-laden sodium alginate (Na-Alg) and $CaCl_2$	Movement speed around 1000 mm/min	21-23 G	Coaxial nozzle printing, flow rate alginate: 0.5-1.5 mL/min	-	Crosslinking via $CaCl_2$ (coaxial nozzle)	L929 mouse fibroblast	~92.9%	Cell viability reduced from 92.9% on day 1 to 67.1% on day 7	(Gao et al., 2015)
PCL and alginate	Dispensing speed: PCL: 60 Alginate: 1500	PCL: 300 Alginate: 200	PCL: 800 Alginate: 10	PCL: 65-80, Alginate: 10	Partial crosslinking: $CaCl_2$: 170 Full crosslinking after fabrication: $CaCl_2$: 100	Rounded and fibroblastic cells isolated from primary cultures of embryonic chick chondrocytes	Minimum viability of 77% for both types of cells during 14 days	Up to 14 days of culture	(Izadifar et al., 2016)
PCL and alginate	Scan velocity: PCL: 80 Alginate: 400	PCL: 250 Alginate: 250	PCL: 650 Alginate: 9-20	PCL: 80 Alginate: room temperature	$CaCl_2$: 100 NaCl: 145	Chondrocyte	~85%	Over 10 days	(Kundu et al., 2015b)

PCL and alginate	Scan velocity: 450	Outer diameter: Alginate: 310, PCL: 350	Alginate: 220 ± 10 PCL: 350 ± 5	Alginate: 26 PCL: 130	Before cell loading: 0.5 wt% $CaCl_2$, after printing: 2 wt% $CaCl_2$	MC3T3-E	~84%	During 7 days	(Lee et al., 2013)
Alginate/ HA	Scan velocity: 240	100	120	-	$CaCl_2$: 100 0.1% w/v polyethylenimine	RSC96 cells (ATTC), an immortalized rat Schwann cell line	83.2%	Over 3 weeks	(Rajaram et al., 2014)
Oxidized alginate, gelatin	Scan velocity: 600-3600	200	55 and 100	37	$CaCl_2$: 100	MG-63 osteoblast	Not reported statistically; high number of living cells	After the plotting process; 5 h of incubation	(Zehnder et al., 2015)

5. Current challenges and the future of hybrid scaffolds

Dispensing-based 3D bioprinting has revolutionized TE with respect to printing artificial tissues and organs but it is not free from limitations. Challenges remain with respect to fabricating hybrid scaffolds, such as the inclusion of vessel-like hollow channels/vascular networks and creation of scaffolds with geometrical features similar to those of native tissues. The following subsections present current limitations, solutions, and future directions.

5.1- Challenges in the design of large hybrid scaffolds using imaging techniques

Successful regeneration of bone, cartilage, and muscle have been reported using conventional TE (Amini et al., 2012; Ostrovidov et al., 2014). However, achieving reproducible and complex constructs together with vascular networks is a major challenge that limits future clinical use (Atala et al., 2012; Mikos et al., 2006). Various biological structures have been fabricated with 3D bioprinting techniques. However, the complexities of microstructures and the 3D anisotropy need to be considered when mimicking native tissues (Hinton et al., 2015). A novel bioprinting system called an integrated tissue and organ printing system has recently been developed to fabricate human-scale tissues with complex constructs and vascularized networks (Kang et al., 2016). Bioprinting techniques require further improvements to fabricate hybrid scaffolds because, in the majority of cases, only simple square lattices are fabricated. These

structures cannot recreate the microstructure of real tissues (Hinton et al., 2015). In this regard, the feasibility of ear regeneration, as a tissue with a complex structure, via 3D printing technique has been demonstrated (J.-S. Lee et al., 2014). However, only acellular hydrogels were used for fabricating the ear-shaped construct because cell viability drops significantly during the fabrication of a large scaffold.

While the combination of imaging and 3D bioprinting techniques has recently facilitated the fabrication of customized hybrid scaffolds, only a few studies have been conducted. For instance, Izadifar et al. tried to scale up the fabrication of hybrid scaffolds including PCL and cell-laden alginate hydrogels. They fabricated cubic scaffolds resembling the thickness of mature cartilage tissue (Izadifar et al., 2016). Moreover, many factors, such as the importance of sacrificial support, should be taken into consideration during the printing of hybrid scaffolds with human-scale sizes. Another factor is the accuracy of the images used to print customized scaffolds. Because medical images are processed to create the CAD files sent to the 3D bioprinter, the accuracy of the final generated file has a decisive role (Naghieh et al., 2016b). Readers are directed elsewhere to review papers on the accuracy of converting image data (Huotilainen et al., 2014; Rengier et al., 2010).

Developing custom-made hybrid scaffolds can accelerate the translation of 3D bioprinting into clinical applications with the assistance of imaging techniques. However, more research is needed with respect to printing complex structures with the assistance of sacrificial support in which the removal process does not affect cell viability. More studies are also needed to improve the accuracy of converting imaging data into 3D models with respect to printing tissues with a complex structure. Further, more *in vivo* studies are required to evaluate the competence of tissue regeneration in large and complex hybrid scaffolds.

5.2- Challenges in technical and printability aspects

Technical challenges include increasing the speed and resolution of biofabrication and the possibility of printing biocompatible materials. As depicted in Table 4, printing parameters and conditions significantly affect cell viability in the bioprinted strand. In a 3D bioprinting system, the viscosity of the biopolymer is a critical factor that needs to be considered to achieve superior printability and printing resolution. Because the viscosity of some polymers is associated with their

concentration in solution, selection of higher viscosity materials requires the application of more concentrated biopolymer during biofabrication. However, a number of studies demonstrate the adverse effect of more concentrated biopolymers on tissue culture. For example, 4% alginate gels regenerated better cartilaginous tissue than 6% alginate gels (Kundu et al., 2015a).

Other vital factors are the crosslinking and stability of hydrogels after fabrication. Although crosslinking is a good method to improve the stability of hydrogels, it is not reproducible (Lee et al., 2013). Several studies reported excessive crosslinking causing a significant reduction in cell viability in biofabrication (Ahn et al., 2012). In addition, the type and concentration of crosslinkers regulate printing parameters (dispensing pressure, needle speed) and the mechanical properties of the resulting 3D scaffolds. Therefore, the choice of crosslinkers and determining an appropriate concentration are critical challenges that need to be addressed. A viscous biomaterial used for 3D cell printing should have good printability while ensuring that its chemical/physical crosslinking does not adversely influence cell viability.

5.3- Development of novel biomaterials for improved biological and/or mechanical properties

The range of biomaterials used in bioprinting is limited and includes natural polymers (collagen, hyaluronic acid, alginate, etc.) as well as synthetic ones (PCL, polylactic acid, polyglycolic acid, etc.). The ideal 3D complex tissue or organ has yet to be printed; the incorporation of cells in hydrogels that have poor mechanical properties is the main obstacle. Thus, researchers have used synthetic biomaterials to improve the mechanical stability of hydrogels (Censi et al., 2011; Fedorovich et al., 2011b). The mechanism by which synthetic materials transfer mechanical stimuli to the encapsulated cells in the hydrogel is complex and requires more investigation. PCL, a synthetic polymer, has been used in some studies to improve the mechanical properties of hybrid structures (Schuurman et al., 2011). However, the role of synthetic polymers in transferring customized mechanical stimuli to the cells encapsulated in hydrogels is important and should be addressed in future studies. Modulating the mechanical properties of a hybrid scaffold to match the structure of native tissues is another critical factor.

A number of biopolymers demonstrate superior printability but lack bioactive molecules in their structure. For example, sodium alginate demonstrates biocompatibility, low toxicity, and printability, and has frequently been used in 3D biopinting (Ahn et al., 2015; Andersen et al., 2015;

Perez et al., 2013). In spite of many attractive features, the deficiency of cell binding moieties on the molecular chain limits the application of sodium alginate; as it has no bioactive proteins (Shim et al., 2012). In this regard, carbodiimmide chemistry is useful in forming a covalent bond between various peptides and alginate molecule (Bettinger et al., 2006). Another biological issue is that cell-laden soft hydrogels degrade faster than synthetic materials in hybrid scaffolds. This non-uniform degradation affects the structural integrity of hybrid scaffolds within a short time during *in vivo* or *in vitro* tissue culture. Moreover, it is difficult to create attachments between successive layers of hydrogels and synthetic materials during bioprinting. Finally, synthetic materials take longer to degrade after *in vivo* implantation and result in inflammation and other biological complexities.

From the mechanical point of view, successful cell-laden hydrogel strands can generally be printed with synthetic polymers (e.g., PCL) to improve the mechanical properties of hybrid scaffolds. However, the heat transferred from the printed synthetic polymers to the hydrogel filaments significantly reduces cell viability (Lee et al., 2017). To limit such detrimental effects of synthetic polymers with a relatively high melting temperature, rapid cooling of PCL has been conducted after dispensing together with a microchannel distance gap between the PCL strands and cells to reduce cell damage in the cell-laden hydrogel (Kang et al., 2016). Another study concluded that PCL printed at 65 to 75 °C did not have any effect on cell viability in the hybrid (PCL/alginate) scaffold due to the quick drop in the surface temperature of the PCL to room temperature (Izadifar et al., 2016). Novel biomaterials should be developed for the fabrication of hybrid scaffolds that overcome the aforementioned limitations. Many efforts have been made to predict the mechanical properties of scaffolds using finite element models to reduce the number of time-consuming experiments, for example by developing accurate numerical models (Karamooz Ravari et al., 2015; Naghieh et al., 2016a; Ravari and Kadkhodaei, 2013). Such models can be utilized to predict the mechanical behavior of hybrid scaffolds in future studies.

5.3.1- Challenges in manipulating multiple materials

Once a novel biomaterial is developed, the next question is how to manipulate various biomaterials to fabricate hybrid scaffolds. Control of the spatial distribution of materials is a key issue with respect to the manipulation of multiple materials. The capacity to manipulate multi-materials/cells during scaffold bio-fabrication is critical to mimic the heterogeneous structures of

native tissue/organs. A straightforward approach is to blend multi-materials/cells for deposition to build scaffolds, resulting in hybrid scaffolds and *in situ*-forming hydrogel scaffolds. This approach is challenged by the need to control the spatial distribution of individual materials/cells within the scaffolds created. To address this challenge, the use of multiple dispensers has been applied over the last decade, wherein multiple materials/cells stored in different dispensers are alternatively applied to build the scaffolds. This approach has been successfully utilized to fabricate hybrid scaffolds comprised of a solid 3D synthetic polymer framework to impart mechanical strength and a hydrogel network to encapsulate cells. However, this approach lacks the ability to dispense multi-materials/cells simultaneously in a controllable manner in comparison with the simple blending method. This limitation has been thoroughly addressed elsewhere, using a microfluidic device with a double-coaxial laminar flow as a novel method to manipulate multi-materials/cells (Hiroaki Onoe, Teru Okitsu, Akane Itou, Midori Kato-Negishi, Riho Gojo, Daisuke Kiriya, Koji Sato, Shigenori Miura, Shintaroh Iwanaga, Kaori Kuribayashi-Shigetomi, Yukiko T. Matsunaga, 2013).

5.4- Challenges in cell viability and the creation of activated hybrid scaffolds

In a 3D hybrid scaffold, a large proportion of the encapsulated cell population can experience necrosis due to limited diffusional mass transfer (Fedorovich et al., 2011a; Hong et al., 2011). Consequently, cells encapsulated in a large 3D scaffold cannot survive for a long time. However, Shim et al. report a new approach to ensure the availability of interconnected pores within a few hundred microns (Shim et al., 2012). Furthermore, because shear-induced cell damage is a common phenomenon in dispensing-based 3D bioprinting, more efforts are required to improve cell viability in this technology (Dababneh and Ozbolat, 2014; Koo and Kim, 2016; Murphy and Atala, 2014). To address this issue, tapered needles have been introduced to reduce shear stress (Ning and Chen, 2017).

As mentioned above, a fundamental challenge in TE is vascularizing a large 3D cellular scaffold printed by a 3D bioprinting technique (Kang et al., 2016; Zhu et al., 2016). Because nutrient diffusion to cells without any vascular network is inefficient beyond a distance of 100 to 200 μm (Kang et al., 2016), cell viability in the scaffold is significantly reduced during *in vivo* or *in vitro* culture. In particular, new blood vessels take a considerable amount of time to grow into scaffolds by angiogenesis/vasculogenesis and this delay remarkably reduces the cell viability due to hypoxia and necrosis (Laschke et al., 2009). Several strategic approaches have been considered

to address this issue. Hollow channels prepared by sacrificial biomaterials have been perfused with endothelial cells to form blood vessels (Miller et al., 2012); the use of a coaxial nozzle to manage the flow of the hydrogel and crosslinker is another possibility to create 3D vasculture (Zhang et al., 2013). Moreover, a multi-nozzle bioprinter was used to fabricate complex tissue and a vascular network layer-by-layer to mimic native tissue (Wang et al., 2016). In this regard, a co-axial nozzle was used to print tubular vascular networks, while a micro nozzle printed cells to fabricate large-scale vascularized tissues. Similarly, fibroblast tissue ligaments together with the vasculature network were printed (Yu et al., 2014). Further, growth factors have been used to stimulate angiogenesis and create a vascular network (Lee et al., 2009; Y.-B. Lee et al., 2010). Another remaining challenge in creating vascular networks is the generation of perfusable prevascularized tissues (Y. S. Zhang et al., 2017). In this regard, *in vivo*/*in vitro* prevascularization was reported to be an effective approach in vasculature formation prior to *in vivo* implantation (Rouwkema et al., 2008). Finally, in addition to the importance of vascular networks in cell viability, fabrication parameters (e.g., applied pressure) can affect cell viability and therefore more investigations are needed to determine optimal fabrication parameters for different biomaterials.

6. Conclusions

Dispensing-based 3D bioprinting techniques have been widely used in the fabrication of tissue scaffolds with living cells, where hydrogels are regarded as the dominant biomaterials. Notably, poor mechanical/biological properties of hydrogels have led researchers to develop hybrid scaffolds from two or more biomaterials with distinct yet complementary properties. Many efforts have been made to address various challenges in the development of hybrid scaffolds with significant advances in terms of their design and fabrication. In terms of fabrication, one common trend to manipulate biomaterials is using multiple dispensers to deposit different biomaterials with dissimilar rheological properties and fabrication conditions (dissolution and crosslinking/gelation aspects). Challenges remain with respect to making attachments between successive layers printed with different biomaterials as well as determining appropriate fabrication parameters to achieve printability with geometric precision. In terms of design, critical issues are associated with the medical imaging used to fabricate customized patient-specific hybrid scaffolds, biomaterials, and the physical architecture of hybrid scaffolds with tailorable mechanical properties. This review highlights the technical (speed and resolution) and printability aspects, development of novel

biomaterials, and fabrication of scaffolds with improved biological and mechanical properties. Many experimental and numerical studies have calculated/predicted the mechanical behavior of hybrid scaffolds and some advancements have occurred with respect to manipulating multiple materials, improving cell viability, creating vessel-like hollow channels/vascular networks, and fabricating large hybrid scaffolds. In spite of many successful achievements, more studies are needed to develop a range of printable biomaterials with appropriate biomechanical properties to create large hybrid scaffolds with vascular networks. The success of printing artificial tissues and organs with hybrid structures lies in the creation of an appropriate microenvironment in which a large cell population can function in an organized fashion to form respective tissues in the presence of a functional vasculature. In the near future, dispensing-based methods to produce bioprinted hybrid scaffolds are predicted to evolve further towards the goal of printing entire organs or damaged tissues.

Acknowledgements

We acknowledge financial support from the Natural Sciences and Engineering Research Council of Canada (NSERC). Furthermore, discussions with Dr. Adam D. McInnes are acknowledged and appreciated.

Author Disclosure Statement

The authors declare no conflict of interest.

References

Addamay123, 2017. Human ear [WWW Document]. URL https://www.thingiverse.com/thing:304657, date of access: June 2017

Ahn, S., Lee, H., Bonassar, L.J., Kim, G., 2012. Cells (MC3T3-E1)-laden alginate scaffolds fabricated by a modified solid-freeform fabrication process supplemented with an aerosol spraying. Biomacromolecules 13, 2997–3003.

Ahn, S.H., Lee, H.J., Lee, J.-S., Yoon, H., Chun, W., Kim, G.H., 2015. A novel cell-printing method and its application to hepatogenic differentiation of human adipose stem cell-embedded mesh structures. Sci. Rep. 5, 13427.

Albrecht, L.D., Sawyer, S.W., Soman, P., 2016. Developing 3D Scaffolds in the Field of Tissue Engineering to Treat Complex Bone Defects. 3D Print. Addit. Manuf. 3, 106–112.

Amini, A.R., Laurencin, C.T., Nukavarapu, S.P., 2012. Bone tissue engineering: recent advances and challenges. Crit. Rev. Biomed. Eng. 40.

Andersen, T., Auk-Emblem, P., Dornish, M., 2015. 3D cell culture in alginate hydrogels. Microarrays 4, 133–161.

Andersson, H., Van Den Berg, A., 2004. Microfabrication and microfluidics for tissue engineering: state of the art and future opportunities. Lab Chip 4, 98–103.

Atala, A., Bauer, S.B., Soker, S., Yoo, J.J., Retik, A.B., 2006. Tissue-engineered autologous bladders for patients needing cystoplasty. Lancet 367, 1241–1246.

Atala, A., Kasper, F.K., Mikos, A.G., 2012. Engineering complex tissues. Sci. Transl. Med. 4, 160rv12-160rv12.

Augst, A.D., Kong, H.J., Mooney, D.J., 2006. Alginate hydrogels as biomaterials. Macromol. Biosci. 6, 623–633.

Bae, H., Puranik, A.S., Gauvin, R., Edalat, F., Carrillo-Conde, B., Peppas, N.A., Khademhosseini, A., 2012. Building vascular networks. Sci. Transl. Med. 4, 160ps23-160ps23.

Bettinger, C.J., Weinberg, E.J., Kulig, K.M., Vacanti, J.P., Wang, Y., Borenstein, J.T., Langer, R., 2006. Three-Dimensional Microfluidic Tissue-Engineering Scaffolds Using a Flexible Biodegradable Polymer. Adv. Mater. 18, 165–169.

Bhattacharjee, T., Zehnder, S.M., Rowe, K.G., Jain, S., Nixon, R.M., Sawyer, W.G., Angelini, T.E., 2015. Writing in the granular gel medium. Sci. Adv. 1, e1500655.

Boccardi, E., Belova, I. V, Murch, G.E., Boccaccini, A.R., Fiedler, T., 2015. Oxygen diffusion in marine-derived tissue engineering scaffolds. J. Mater. Sci. Mater. Med. 26, 1–9.

Bohari, S.P.M., Hukins, D.W.L., Grover, L.M., 2011. Effect of calcium alginate concentration on viability and proliferation of encapsulated fibroblasts. Biomed. Mater. Eng. 21, 159–170. doi:10.3233/BME-2011-0665

Boucard, N., Viton, C., Agay, D., Mari, E., Roger, T., Chancerelle, Y., Domard, A., 2007. The use of physical hydrogels of chitosan for skin regeneration following third-degree burns. Biomaterials 28, 3478–3488.

Cazon, A., Aizpurua, J., Paterson, A., Bibb, R., Campbell, R.I., 2014. Customised design and manufacture of protective face masks combining a practitioner-friendly modelling approach and low-cost devices for digitising and additive manufacturing. Virtual Phys. Prototyp. 9, 251–261.

Cebotari, S., Lichtenberg, A., Tudorache, I., Hilfiker, A., Mertsching, H., Leyh, R., Breymann, T., Kallenbach, K., Maniuc, L., Batrinac, A., 2006. Clinical application of tissue engineered human heart valves using autologous progenitor cells. Circulation 114, I-132.

Censi, R., Schuurman, W., Malda, J., Di Dato, G., Burgisser, P.E., Dhert, W.J.A., Van Nostrum, C.F., Di

Martino, P., Vermonden, T., Hennink, W.E., 2011. A Printable Photopolymerizable Thermosensitive p (HPMAm-lactate)-PEG Hydrogel for Tissue Engineering. Adv. Funct. Mater. 21, 1833–1842.

Chen, X.B., Li, M.G., Ke, H., 2008. Modeling of the Flow Rate in the Dispensing-Based Process for Fabricating Tissue Scaffolds. J. Manuf. Sci. Eng. 130, 21003. doi:10.1115/1.2789725

Christensen, K., Xu, C., Chai, W., Zhang, Z., Fu, J., Huang, Y., 2015. Freeform inkjet printing of cellular structures with bifurcations. Biotechnol. Bioeng. 112, 1047–1055.

Chrobak, K.M., Potter, D.R., Tien, J., 2006. Formation of perfused, functional microvascular tubes in vitro. Microvasc. Res. 71, 185–196.

Cohen, D.L., Malone, E., Lipson, H.O.D., Bonassar, L.J., 2006. Direct freeform fabrication of seeded hydrogels in arbitrary geometries. Tissue Eng. 12, 1325–1335.

Correlo, V.M., Boesel, L.F., Pinho, E., Costa-Pinto, A.R., Alves da Silva, M.L., Bhattacharya, M., Mano, J.F., Neves, N.M., Reis, R.L., 2009. Melt-based compression-molded scaffolds from chitosan–polyester blends and composites: Morphology and mechanical properties. J. Biomed. Mater. Res. Part A 91, 489–504.

Cui, X., Breitenkamp, K., Finn, M.G., Lotz, M., D'Lima, D.D., 2012. Direct human cartilage repair using three-dimensional bioprinting technology. Tissue Eng. Part A 18, 1304–1312.

da Silva Oliveira Brito, N.M., de Souza Coelho Soares, R., Lafitt Tavares Monteiro, E., Charifker Ribeiro Martins, S., Raimundo Cavalcante, J., Grotta Grempel, R., de Oliveira Neto, J.A., 2016. Additive Manufacturing for Surgical Planning of Mandibular Fracture. Acta Stomatol. Croat. 50, 348–353. doi:10.15644/asc50/4/8

Dababneh, A.B., Ozbolat, I.T., 2014. Bioprinting technology: a current state-of-the-art review. J. Manuf. Sci. Eng. 136, 61016.

Datta, P., Ayan, B., Ozbolat, I.T., 2017. Bioprinting for vascular and vascularized tissue biofabrication. Acta Biomater. 51, 1–20. doi:10.1016/j.actbio.2017.01.035

Dhoot, N.O., Tobias, C.A., Fischer, I., Wheatley, M.A., 2004. Peptide-modified alginate surfaces as a growth permissive substrate for neurite outgrowth. J. Biomed. Mater. Res. Part A 71, 191–200.

Duan, B., Hockaday, L.A., Kang, K.H., Butcher, J.T., 2013. 3D bioprinting of heterogeneous aortic valve conduits with alginate/gelatin hydrogels. J. Biomed. Mater. Res. Part A 101, 1255–1264.

El-Ayoubi, R., DeGrandpré, C., DiRaddo, R., Yousefi, A.-M., Lavigne, P., 2011. Design and dynamic culture of 3D-scaffolds for cartilage tissue engineering. J. Biomater. Appl. 25, 429–444.

El-Ayoubi, R., Eliopoulos, N., Diraddo, R., Galipeau, J., Yousefi, A.-M., 2008. Design and fabrication of 3D porous scaffolds to facilitate cell-based gene therapy. Tissue Eng. Part A 14, 1037–1048.

England, S., Rajaram, A., Schreyer, D.J., Chen, X., 2016. Bioprinted fibrin-factor XIII-hyaluronate

hydrogel scaffolds with encapsulated Schwann cells and their in vitro characterization for use in nerve regeneration. Bioprinting 1–9. doi:10.1016/j.bprint.2016.12.001

Eyrich, D., Wiese, H., Maier, G., Skodacek, D., Appel, B., Sarhan, H., Tessmar, J., Staudenmaier, R., Wenzel, M.M., Goepferich, A., 2007. In vitro and in vivo cartilage engineering using a combination of chondrocyte-seeded long-term stable fibrin gels and polycaprolactone-based polyurethane scaffolds. Tissue Eng. 13, 2207–2218.

Fedorovich, N.E., De Wijn, J.R., Verbout, A.J., Alblas, J., Dhert, W.J.A., 2008. Three-dimensional fiber deposition of cell-laden, viable, patterned constructs for bone tissue printing. Tissue Eng. Part A 14, 127–133.

Fedorovich, N.E., Kuipers, E., Gawlitta, D., Dhert, W.J.A., Alblas, J., 2011a. Scaffold porosity and oxygenation of printed hydrogel constructs affect functionality of embedded osteogenic progenitors. Tissue Eng. Part A 17, 2473–2486.

Fedorovich, N.E., Schuurman, W., Wijnberg, H.M., Prins, H.-J., van Weeren, P.R., Malda, J., Alblas, J., Dhert, W.J.A., 2011b. Biofabrication of osteochondral tissue equivalents by printing topologically defined, cell-laden hydrogel scaffolds. Tissue Eng. Part C Methods 18, 33–44.

Ferris, C.J., Gilmore, K.G., Wallace, G.G., 2013. Biofabrication: an overview of the approaches used for printing of living cells. Appl. Microbiol. Biotechnol. 97, 4243–4258.

Fierz, F.C., Beckmann, F., Huser, M., Irsen, S.H., Leukers, B., Witte, F., Degistirici, Ö., Andronache, A., Thie, M., Müller, B., 2008. The morphology of anisotropic 3D-printed hydroxyapatite scaffolds. Biomaterials 29, 3799–3806.

Gao, Q., He, Y., Fu, J., Liu, A., Ma, L., 2015. Coaxial nozzle-assisted 3D bioprinting with built-in microchannels for nutrients delivery. Biomaterials 61, 203–215. doi:10.1016/j.biomaterials.2015.05.031

Gloria, A., Causa, F., De Santis, R., Netti, P.A., Ambrosio, L., 2007. Dynamic-mechanical properties of a novel composite intervertebral disc prosthesis. J. Mater. Sci. Mater. Med. 18, 2159–2165.

Guillemot, F., Souquet, A., Catros, S., Guillotin, B., Lopez, J., Faucon, M., Pippenger, B., Bareille, R., Rémy, M., Bellance, S., 2010. High-throughput laser printing of cells and biomaterials for tissue engineering. Acta Biomater. 6, 2494–2500.

Guillotin, B., Souquet, A., Catros, S., Duocastella, M., Pippenger, B., Bellance, S., Bareille, R., Rémy, M., Bordenave, L., Amédée, J., 2010. Laser assisted bioprinting of engineered tissue with high cell density and microscale organization. Biomaterials 31, 7250–7256.

Hayami, J.W.S., Surrao, D.C., Waldman, S.D., Amsden, B.G., 2010. Design and characterization of a biodegradable composite scaffold for ligament tissue engineering. J. Biomed. Mater. Res. Part A 92, 1407–1420.

Highley, C.B., Rodell, C.B., Burdick, J.A., 2015. Direct 3D printing of shear-thinning hydrogels into self-healing hydrogels. Adv. Mater. 27, 5075–5079.

Hinton, T.J., Jallerat, Q., Palchesko, R.N., Park, J.H., Grodzicki, M.S., Shue, H., Ramadan, M.H., Hudson, A.R., Feinberg, A.W., 2015. Three-dimensional printing of complex biological structures by freeform reversible embedding of suspended hydrogels. Sci. Adv. 1, 1–10. doi:10.1126/sciadv.1500758

Hinton, T.J., Lee, A., Feinberg, A.W., 2017. 3D Bioprinting from the Micrometer to Millimeter Length Scales: Size Does Matter. Curr. Opin. Biomed. Eng. doi:10.1016/j.cobme.2017.02.004

Hiroaki Onoe, Teru Okitsu, Akane Itou, Midori Kato-Negishi, Riho Gojo, Daisuke Kiriya, Koji Sato, Shigenori Miura, Shintaroh Iwanaga, Kaori Kuribayashi-Shigetomi, Yukiko T. Matsunaga, Y.S. and S.T., 2013. Metre-long cell-laden microfibres exhibit tissue morphologies and functions. Nat. Mater. 12, 584–590.

Hockaday, L.A., Kang, K.H., Colangelo, N.W., Cheung, P.Y.C., Duan, B., Malone, E., Wu, J., Girardi, L.N., Bonassar, L.J., Lipson, H., 2012. Rapid 3D printing of anatomically accurate and mechanically heterogeneous aortic valve hydrogel scaffolds. Biofabrication 4, 35005.

Hoffman, A.S., 2012. Hydrogels for biomedical applications. Adv. Drug Deliv. Rev. 64, 18–23.

Holloway, J.L., Lowman, A.M., Palmese, G.R., 2010. Mechanical evaluation of poly (vinyl alcohol)-based fibrous composites as biomaterials for meniscal tissue replacement. Acta Biomater. 6, 4716–4724.

Hölzl, K., Lin, S., Tytgat, L., Van Vlierberghe, S., Gu, L., Ovsianikov, A., 2016. Bioink properties before, during and after 3D bioprinting. Biofabrication 8, 32002. doi:10.1088/1758-5090/8/3/032002

Hon, K.K.B., Li, L., Hutchings, I.M., 2008. Direct writing technology—Advances and developments. CIRP Ann. Technol. 57, 601–620.

Hong, S.J., Jin, D.P., Buck, D.W., Galiano, R.D., Mustoe, T.A., 2011. Impaired response of mature adipocytes of diabetic mice to hypoxia. Exp. Cell Res. 317, 2299–2307.

Huang, Y., He, K., Wang, X., 2013. Rapid prototyping of a hybrid hierarchical polyurethane-cell/hydrogel construct for regenerative medicine. Mater. Sci. Eng. C 33, 3220–3229.

Huotilainen, E., Jaanimets, R., Valášek, J., Marcián, P., Salmi, M., Tuomi, J., Mäkitie, A., Wolff, J., 2014. Inaccuracies in additive manufactured medical skull models caused by the DICOM to STL conversion process. J. Cranio-Maxillofacial Surg. 42, e259–e265. doi:10.1016/j.jcms.2013.10.001

Hutmacher, D.W., Sittinger, M., Risbud, M. V, 2004. Scaffold-based tissue engineering: rationale for computer-aided design and solid free-form fabrication systems. Trends Biotechnol. 22, 354–362. doi:http://dx.doi.org/10.1016/j.tibtech.2004.05.005

Izadifar, M., 2013. Biomanufacturing versus superficial cell seeding: simulation of chondrocyte proliferation in a cylindrical cartilage scaffold. Int. J. Tissue Eng. 2013.

Izadifar, M., Babyn, P., Kelly, M.E., Chapman, D., Chen, X., 2017. Bioprinting pattern-dependent electrical/mechanical behavior of cardiac alginate implants: characterization and ex-vivo phase-contrast microtomography assessment. Tissue Eng.

Izadifar, M., Chen, X., 2013. Radio frequency heating of implanted tissue engineered scaffolds: simulation and experimental studies. Front. Heat Mass Transf. 3.

Izadifar, Z., Chang, T., Kulyk, W.M., Chen, D., Eames, B.F., 2016. Analyzing biological performance of 3D-printed, cell-impregnated hybrid constructs for cartilage tissue engineering. Tissue Eng. Part C. Methods 22, 173–188. doi:10.1089/ten.TEC.2015.0307

Izadifar, Z., Chen, X., Kulyk, W., 2012. Strategic design and fabrication of engineered scaffolds for articular cartilage repair. J. Funct. Biomater. 3, 799–838. doi:10.3390/jfb3040799

Jia, W., Gungor-Ozkerim, P.S., Zhang, Y.S., Yue, K., Zhu, K., Liu, W., Pi, Q., Byambaa, B., Dokmeci, M.R., Shin, S.R., Khademhosseini, A., 2016. Direct 3D bioprinting of perfusable vascular constructs using a blend bioink. Biomaterials 106, 58–68. doi:10.1016/j.biomaterials.2016.07.038

Jung, Y., Kim, S.-H., Kim, Y.H., Kim, S.H., 2010. The effect of hybridization of hydrogels and poly (L-lactide-co-ε-caprolactone) scaffolds on cartilage tissue engineering. J. Biomater. Sci. Polym. Ed. 21, 581–592.

Kang, H., Lee, S.J., Ko, I.K., Kengla, C., Yoo, J.J., Atala, A., 2016. A 3D bioprinting system to produce human-scale tissue constructs with structural integrity. Nat. Biotechnol. 34, 312–319. doi:10.1038/nbt.3413

Karamooz Ravari, M.R., Kadkhodaei, M., Ghaei, A., 2015. Effects of asymmetric material response on the mechanical behavior of porous shape memory alloys. J. Intell. Mater. Syst. Struct. doi:10.1177/1045389X15604232

Kawazoe, N., Inoue, C., Tateishi, T., Chen, G., 2010. A cell leakproof PLGA-collagen hybrid scaffold for cartilage tissue engineering. Biotechnol. Prog. 26, 819–826.

Khalil, S., Sun, W., 2007. Biopolymer deposition for freeform fabrication of hydrogel tissue constructs. Mater. Sci. Eng. C 27, 469–478.

Kim, J.J., Hou, L., Huang, N.F., 2016. Vascularization of three-dimensional engineered tissues for regenerative medicine applications. Acta Biomater. 41, 17–26. doi:10.1016/j.actbio.2016.06.001

Kim, M., Jo, S.B., Park, J.H., Cho, K., 2015. Flexible lateral organic solar cells with core–shell structured organic nanofibers. Nano Energy 18, 97–108.

Kim, T.G., Chung, H.J., Park, T.G., 2008. Macroporous and nanofibrous hyaluronic acid/collagen hybrid scaffold fabricated by concurrent electrospinning and deposition/leaching of salt particles. Acta

Biomater. 4, 1611–1619.

Kishan, A.P., Robbins, A.B., Mohiuddin, S.F., Jiang, M., Moreno, M.R., Cosgriff-Hernandez, E.M., 2016. Fabrication of macromolecular gradients in aligned fiber scaffolds using a combination of in-line blending and air-gap electrospinning. Acta Biomater.

Klein, T.J., Malda, J., Sah, R.L., Hutmacher, D.W., 2009. Tissue engineering of articular cartilage with biomimetic zones. Tissue Eng. Part B Rev. 15, 143–157.

Koo, Y., Kim, G., 2016. New strategy for enhancing in situ cell viability of cell-printing process via piezoelectric transducer-assisted three-dimensional printing. Biofabrication 8, 25010.

Kundu, J., Shim, J.-H., Jang, J., Kim, S.-W., Cho, D.-W., 2015a. An additive manufacturing-based PCL-alginate-chondrocyte bioprinted scaffold for cartilage tissue engineering. J. Tissue Eng. Regen. Med. 9, 1286–1297. doi:10.1002/term.1682

Kundu, J., Shim, J.H., Jang, J., Kim, S.W., Cho, D.W., 2015b. An additive manufacturing-based PCL-alginate-chondrocyte bioprinted scaffold for cartilage tissue engineering. J. Tissue Eng. Regen. Med. 9, 1286–1297. doi:10.1002/term.1682

Langer, R., 2009. Perspectives and challenges in tissue engineering and regenerative medicine. Adv. Mater. 21, 3235–3236.

Laschke, M.W., Vollmar, B., Menger, M.D., 2009. Inosculation: connecting the life-sustaining pipelines. Tissue Eng. Part B Rev. 15, 455–465.

Lebourg, M., Serra, R.S., Estellés, J.M., Sánchez, F.H., Ribelles, J.L.G., Antón, J.S., 2008. Biodegradable polycaprolactone scaffold with controlled porosity obtained by modified particle-leaching technique. J. Mater. Sci. Mater. Med. 19, 2047–2053.

Lee, H., Ahn, S., Bonassar, L.J., Kim, G., 2013. Cell (MC3T3-E1)-Printed Poly (ϵ-caprolactone)/Alginate Hybrid Scaffolds for Tissue Regeneration. Macromol. Rapid Commun. 34, 142–149.

Lee, H., Koo, Y.W., Yeo, M., Kim, S., Kim, G.H., 2017. Recent cell printing systems for tissue engineering. Int. J. Bioprinting 3.

Lee, J.-S., Hong, J.M., Jung, J.W., Shim, J.-H., Oh, J.-H., Cho, D.-W., 2014. 3D printing of composite tissue with complex shape applied to ear regeneration. Biofabrication 6, 24103. doi:10.1088/1758-5082/6/2/024103

Lee, V.K., Kim, D.Y., Ngo, H., Lee, Y., Seo, L., Yoo, S.-S., Vincent, P.A., Dai, G., 2014a. Creating perfused functional vascular channels using 3D bio-printing technology. Biomaterials 35, 8092–8102.

Lee, V.K., Lanzi, A.M., Ngo, H., Yoo, S.-S., Vincent, P.A., Dai, G., 2014b. Generation of multi-scale vascular network system within 3D hydrogel using 3D bio-printing technology. Cell. Mol. Bioeng. 7, 460–472.

Lee, W., Debasitis, J.C., Lee, V.K., Lee, J.-H., Fischer, K., Edminster, K., Park, J.-K., Yoo, S.-S., 2009. Multi-layered culture of human skin fibroblasts and keratinocytes through three-dimensional freeform fabrication. Biomaterials 30, 1587–1595.

Lee, W., Lee, V., Polio, S., Keegan, P., Lee, J.-H., Fischer, K., Park, J.-K., Yoo, S.-S., 2010. On-demand three-dimensional freeform fabrication of multi-layered hydrogel scaffold with fluidic channels. Biotechnol. Bioeng. 105, 1178.

Lee, Y.-B., Polio, S., Lee, W., Dai, G., Menon, L., Carroll, R.S., Yoo, S.-S., 2010. Bio-printing of collagen and VEGF-releasing fibrin gel scaffolds for neural stem cell culture. Exp. Neurol. 223, 645–652.

Li, M., Tian, X., Zhu, N., Schreyer, D.J., Chen, X., 2010. Modeling Process-Induced Cell Damage. Tissue Eng. Part C 16.

Li, M.G., Tian, X.Y., Chen, X.B., 2009. A brief review of dispensing-based rapid prototyping techniques in tissue scaffold fabrication: role of modeling on scaffold properties prediction. Biofabrication 1, 32001. doi:10.1088/1758-5082/1/3/032001

Li, S., Xiong, Z., Wang, X., Yan, Y., Liu, H., Zhang, R., 2009a. Direct fabrication of a hybrid cell/hydrogel construct by a double-nozzle assembling technology. J. Bioact. Compat. Polym. 24, 249–265.

Li, S., Yan, Y., Xiong, Z., Zhang, C.W.R., Wang, X., 2009b. Gradient hydrogel construct based on an improved cell assembling system. J. Bioact. Compat. Polym. 24, 84–99.

Lien, S.-M., Ko, L.-Y., Huang, T.-J., 2009. Effect of pore size on ECM secretion and cell growth in gelatin scaffold for articular cartilage tissue engineering. Acta Biomater. 5, 670–679.

Lin, A.S.P., Barrows, T.H., Cartmell, S.H., Guldberg, R.E., 2003. Microarchitectural and mechanical characterization of oriented porous polymer scaffolds. Biomaterials 24, 481–489.

Liu, L., Zhou, X., Xu, Y., Zhang, W., Liu, C.-H., Wang, X., 2015. Controlled release of growth factors for regenerative medicine. Curr. Pharm. Des. 21, 1627–1632.

Liu, Y., Zhang, L., Zhou, G., Li, Q., Liu, W., Yu, Z., Luo, X., Jiang, T., Zhang, W., Cao, Y., 2010. In vitro engineering of human ear-shaped cartilage assisted with CAD/CAM technology. Biomaterials 31, 2176–2183.

Lv, S., Bu, T., Kayser, J., Bausch, A., Li, H., 2013. Towards constructing extracellular matrix-mimetic hydrogels: an elastic hydrogel constructed from tandem modular proteins containing tenascin FnIII domains. Acta Biomater. 9, 6481–6491.

Macaya, D., Spector, M., 2012. Injectable hydrogel materials for spinal cord regeneration: a review. Biomed. Mater. 7, 12001.

Macchiarini, P., Jungebluth, P., Go, T., Asnaghi, M.A., Rees, L.E., Cogan, T.A., Dodson, A., Martorell,

J., Bellini, S., Parnigotto, P.P., 2008. Clinical transplantation of a tissue-engineered airway. Lancet 372, 2023–2030.

Mannoor, M.S., Jiang, Z., James, T., Kong, Y.L., Malatesta, K.A., Soboyejo, W.O., Verma, N., Gracias, D.H., McAlpine, M.C., 2013. 3D printed bionic ears. Nano Lett. 13, 2634.

Manojlovic, V., Djonlagic, J., Obradovic, B., Nedovic, V., Bugarski, B., 2006. Investigations of cell immobilization in alginate: rheological and electrostatic extrusion studies. J. Chem. Technol. Biotechnol. 81, 505–510.

Martin, I., Simmons, P.J., Williams, D.F., 2014. Manufacturing challenges in regenerative medicine. Sci. Transl. Med. 6, 232fs16-232fs16.

Martínez Ávila, H., Schwarz, S., Rotter, N., Gatenholm, P., 2016. 3D bioprinting of human chondrocyte-laden nanocellulose hydrogels for patient-specific auricular cartilage regeneration. Bioprinting 1, 22–35. doi:10.1016/j.bprint.2016.08.003

Martino, M.M., Briquez, P.S., Ranga, A., Lutolf, M.P., Hubbell, J.A., 2013. Heparin-binding domain of fibrin (ogen) binds growth factors and promotes tissue repair when incorporated within a synthetic matrix. Proc. Natl. Acad. Sci. 110, 4563–4568.

Matsumura, G., Hibino, N., Ikada, Y., Kurosawa, H., Shin'oka, T., 2003. Successful application of tissue engineered vascular autografts: clinical experience. Biomaterials 24, 2303–2308.

Matyash, M., Despang, F., Mandal, R., Fiore, D., Gelinsky, M., Ikonomidou, C., 2012. Novel Soft Alginate Hydrogel Strongly Supports Neurite Growth and Protects Neurons Against Oxidative Stress. Tissue Eng. Part A 18, 55–66. doi:10.1089/ten.tea.2011.0097

McMahon, R.E., Qu, X., Jimenez-Vergara, A.C., Bashur, C.A., Guelcher, S.A., Goldstein, A.S., Hahn, M.S., 2011. Hydrogel–electrospun mesh composites for coronary artery bypass grafts. Tissue Eng. Part C Methods 17, 451–461.

Mikos, A.G., Herring, S.W., Ochareon, P., Elisseeff, J., Lu, H.H., Kandel, R., Schoen, F.J., Toner, M., Mooney, D., Atala, A., 2006. Engineering complex tissues. Tissue Eng. 12, 3307–3339.

Miller, J.S., Stevens, K.R., Yang, M.T., Baker, B.M., Nguyen, D.-H.T., Cohen, D.M., Toro, E., Chen, A.A., Galie, P.A., Yu, X., 2012. Rapid casting of patterned vascular networks for perfusable engineered three-dimensional tissues. Nat. Mater. 11, 768–774.

Mironov, V., Kasyanov, V., Drake, C., Markwald, R.R., 2008. Organ printing: promises and challenges. Regen. Med. 3, 93–103.

Mironov, V., Visconti, R.P., Kasyanov, V., Forgacs, G., Drake, C.J., Markwald, R.R., 2009. Organ printing: tissue spheroids as building blocks. Biomaterials 30, 2164–2174.

Moon, S., Hasan, S.K., Song, Y.S., Xu, F., Keles, H.O., Manzur, F., Mikkilineni, S., Hong, J.W., Nagatomi, J., Haeggstrom, E., 2009. Layer by layer three-dimensional tissue epitaxy by cell-laden

hydrogel droplets. Tissue Eng. Part C Methods 16, 157–166.

Moroni, L., De Wijn, J.R., Van Blitterswijk, C.A., 2006. 3D fiber-deposited scaffolds for tissue engineering: influence of pores geometry and architecture on dynamic mechanical properties. Biomaterials 27, 974–985.

Moroni, L., De Wijn, J.R., Van Blitterswijk, C.A., 2005. Three-dimensional fiber-deposited PEOT/PBT copolymer scaffolds for tissue engineering: Influence of porosity, molecular network mesh size, and swelling in aqueous media on dynamic mechanical properties. J. Biomed. Mater. Res. Part A 75, 957–965.

Mota, C., Puppi, D., Chiellini, F., Chiellini, E., 2015. Additive manufacturing techniques for the production of tissue engineering constructs. J. Tissue Eng. Regen. Med. 9, 174–190.

Murphy, S. V, Atala, A., 2014. 3D bioprinting of tissues and organs. Nat. Biotechnol. 32, 773–785. doi:10.1038/nbt.2958

Naghieh, S., Badrossamay, M., Foroozmehr, E., Kharaziha, M., 2017. Combination of PLA Micro-fibers and PCL-Gelatin Nano-fibers for Development of Bone Tissue Engineering Scaffolds. Int. J. Swarm Intell. Evol. Comput. 6, 1–4. doi:10.4172/2090-4908.1000150

Naghieh, S., Foroozmehr, E., Badrossamay, M., Kharaziha, M., 2017. Combinational processing of 3D printing and electrospinning of hierarchical poly(lactic acid)/gelatin-forsterite scaffolds as a biocomposite: Mechanical and biological assessment. Mater. Des. doi:10.1016/j.matdes.2017.07.051

Naghieh, S., Karamooz Ravari, M.R., Badrossamay, M., Foroozmehr, E., Kadkhodaei, M., 2016a. Numerical investigation of the mechanical properties of the additive manufactured bone scaffolds fabricated by FDM: The effect of layer penetration and post-heating. J. Mech. Behav. Biomed. Mater. 59, 241–250. doi:10.1016/j.jmbbm.2016.01.031

Naghieh, S., Reihany, A., Haghighat, A., Foroozmehr, E., Badrossamay, M., Forooghi, F., 2016b. Fused Deposition Modeling and Fabrication of a Three-dimensional Model in Maxillofacial Reconstruction. Regen. Reconstr. Restor. 1, 139–144.

Nair, K., Gandhi, M., Khalil, S., Yan, K.C., Marcolongo, M., Barbee, K., Sun, W., 2009. Characterization of cell viability during bioprinting processes. Biotechnol. J. 4, 1168–1177.

Nakamura, M., Iwanaga, S., Henmi, C., Arai, K., Nishiyama, Y., 2010. Biomatrices and biomaterials for future developments of bioprinting and biofabrication. Biofabrication 2, 14110.

Nerurkar, N.L., Sen, S., Huang, A.H., Elliott, D.M., Mauck, R.L., 2010. Engineered disc-like angle-ply structures for intervertebral disc replacement. Spine (Phila. Pa. 1976). 35, 867.

Nicodemus, G.D., Bryant, S.J., 2008. Cell encapsulation in biodegradable hydrogels for tissue engineering applications. Tissue Eng. Part B Rev. 14, 149–165.

Ning, L.Q., Chen, X.B., 2017. A Brief Review of Extrusion-based Tissue Scaffold Bio-Printing.

Biotechnol. J. 1–47.

Nomi, M., Atala, A., De Coppi, P., Soker, S., 2002. Principals of neovascularization for tissue engineering. Mol. Aspects Med. 23, 463–483.

Norotte, C., Marga, F.S., Niklason, L.E., Forgacs, G., 2009. Scaffold-free vascular tissue engineering using bioprinting. Biomaterials 30, 5910–5917.

Novikova, L.N., Mosahebi, A., Wiberg, M., Terenghi, G., Kellerth, J., Novikov, L.N., 2006. Alginate hydrogel and matrigel as potential cell carriers for neurotransplantation. J. Biomed. Mater. Res. Part A 77, 242–252.

Offeddu, G.S., Ashworth, J.C., Cameron, R.E., Oyen, M.L., 2016. Structural determinants of hydration, mechanics and fluid flow in freeze-dried collagen scaffolds. Acta Biomater. 41, 193–203.

Olubamiji, A.D., Izadifar, Z., Si, J.L., Cooper, D.M.L., Eames, B.F., Chen, D.X., 2016. Modulating mechanical behaviour of 3D-printed cartilage-mimetic PCL scaffolds: influence of molecular weight and pore geometry. Biofabrication 8, 25020. doi:10.1088/1758-5090/8/2/025020

Ostrovidov, S., Hosseini, V., Ahadian, S., Fujie, T., Parthiban, S.P., Ramalingam, M., Bae, H., Kaji, H., Khademhosseini, A., 2014. Skeletal muscle tissue engineering: methods to form skeletal myotubes and their applications. Tissue Eng. Part B Rev. 20, 403–436.

Otton, J.M., Birbara, N.S., Hussain, T., Greil, G., Foley, T.A., Pather, N., 2017. 3D printing from cardiovascular CT : a practical guide and review. Cardiovasc. Diagn. Ther. doi:10.21037/cdt.2017.01.12

Ozbolat, I.T., Yin Yu, 2013. Bioprinting Toward Organ Fabrication: Challenges and Future Trends. IEEE Trans. Biomed. Eng. 60, 691–699. doi:10.1109/TBME.2013.2243912

Pati, F., Shim, J.-H., Lee, J.-S., Cho, D.-W., 2013. 3D printing of cell-laden constructs for heterogeneous tissue regeneration. Manuf. Lett. 1, 49–53.

Perez, R.A., Kim, H.-W., 2015. Core–shell designed scaffolds for drug delivery and tissue engineering. Acta Biomater. 21, 2–19.

Perez, R.A., Kim, M., Kim, T.-H., Kim, J.-H., Lee, J.H., Park, J.-H., Knowles, J.C., Kim, H.-W., 2013. Utilizing core–shell fibrous collagen-alginate hydrogel cell delivery system for bone tissue engineering. Tissue Eng. Part A 20, 103–114.

Purcell, B.P., Lobb, D., Charati, M.B., Dorsey, S.M., Wade, R.J., Zellars, K.N., Doviak, H., Pettaway, S., Logdon, C.B., Shuman, J.A., 2014. Injectable and bioresponsive hydrogels for on-demand matrix metalloproteinase inhibition. Nat. Mater. 13, 653–661.

Rajaram, A., Chen, X.-B., Schreyer, D.J., 2012. Strategic Design and Recent Fabrication Techniques for Bioengineered Tissue Scaffolds to Improve Peripheral Nerve Regeneration. Tissue Eng. Part B Rev. 18, 454–467. doi:10.1089/ten.teb.2012.0006

Rajaram, A., Schreyer, D., Chen, D., 2014. Bioplotting Alginate / Hyaluronic Acid Hydrogel Scaffolds with Structural Integrity and Preserved Schwann Cell Viability. 3D Print. 1, 194–203. doi:10.1089/3dp.2014.0006

Ravari, M.R.K., Kadkhodaei, M., 2013. Finite element modeling of the elastic modulus of Ti6al4v scaffold fabricated by SLM, in: Poromechanics V5, Proceedings of the Fifth Biot Conference on Poromechanics. pp. 1021–1028.

Rengier, F., Mehndiratta, A., von Tengg-Kobligk, H., Zechmann, C.M., Unterhinninghofen, R., Kauczor, H.-U., Giesel, F.L., 2010. 3D printing based on imaging data: review of medical applications. Int. J. Comput. Assist. Radiol. Surg. 5, 335–341.

Ricci, J.L., Clark, E.A., Murriky, A., Smay, J.E., 2012. Three-dimensional printing of bone repair and replacement materials: impact on craniofacial surgery. J. Craniofac. Surg. 23, 304–308.

Richards, D., Jia, J., Yost, M., Markwald, R., Mei, Y., 2017. 3D bioprinting for vascularized tissue fabrication. Ann. Biomed. Eng. 45, 132–147.

Rouwkema, J., Khademhosseini, A., 2016. Vascularization and Angiogenesis in Tissue Engineering: Beyond Creating Static Networks. Trends Biotechnol. 34, 733–745. doi:10.1016/j.tibtech.2016.03.002

Rouwkema, J., Rivron, N.C., van Blitterswijk, C.A., 2008. Vascularization in tissue engineering. Trends Biotechnol. 26, 434–441.

Santos, L., Fuhrmann, G., Juenet, M., Amdursky, N., Horejs, C., Campagnolo, P., Stevens, M.M., 2015. Extracellular stiffness modulates the expression of functional proteins and growth factors in endothelial cells. Adv. Healthc. Mater. 4, 2056–2063.

Sarker, M., Chen, X.B., 2017. Modeling the flow behavior and flow rate of medium viscosity alginate for scaffold fabrication with a 3D bioplotter.

Sarker, M., Chen, X.B., Schreyer, D.J., 2015. Experimental approaches to vascularisation within tissue engineering constructs. J. Biomater. Sci. Polym. Ed. 26, 683–734. doi:10.1080/09205063.2015.1059018

Schagemann, J.C., Chung, H.W., Mrosek, E.H., Stone, J.J., Fitzsimmons, J.S., O'driscoll, S.W., Reinholz, G.G., 2010. Poly-ϵ-caprolactone/gel hybrid scaffolds for cartilage tissue engineering. J. Biomed. Mater. Res. Part A 93, 454–463.

Schuurman, W., Khristov, V., Pot, M.W., van Weeren, P.R., Dhert, W.J. a, Malda, J., 2011. Bioprinting of hybrid tissue constructs with tailorable mechanical properties. Biofabrication 3, 1–7. doi:10.1088/1758-5082/3/2/021001

Sekine, H., Shimizu, T., Yang, J., Kobayashi, E., Okano, T., 2006. Pulsatile myocardial tubes fabricated with cell sheet engineering. Circulation 114, I-87.

Seol, Y.-J., Kang, H.-W., Lee, S.J., Atala, A., Yoo, J.J., 2014. Bioprinting technology and its applications. Eur. J. Cardio-Thoracic Surg. ezu148.

Shah, A.M., Jung, H., Skirboll, S., 2014. Materials used in cranioplasty: a history and analysis. Neurosurg. Focus 36, E19.

Shamloo, A., Heilshorn, S.C., 2010. Matrix density mediates polarization and lumen formation of endothelial sprouts in VEGF gradients. Lab Chip 10, 3061–3068.

Shim, J.-H., Kim, J.Y., Park, M., Park, J., Cho, D.-W., 2011. Development of a hybrid scaffold with synthetic biomaterials and hydrogel using solid freeform fabrication technology. Biofabrication 3, 34102.

Shim, J.-H., Lee, J., Kim, J.Y., Cho, D.-W., 2012. Bioprinting of a mechanically enhanced three-dimensional dual cell-laden construct for osteochondral tissue engineering using a multi-head tissue/organ building system. J. Micromechanics Microengineering 22, 85014. doi:10.1088/0960-1317/22/8/085014

Spiteri, C.G., Pilliar, R.M., Kandel, R.A., 2006. Substrate porosity enhances chondrocyte attachment, spreading, and cartilage tissue formation in vitro. J. Biomed. Mater. Res. Part A 78, 676–683.

Sui, S., Wang, X., Liu, P., Yan, Y., Zhang, R., 2009. Cryopreservation of cells in 3D constructs based on controlled cell assembly processes. J. Bioact. Compat. Polym. 24, 473–487.

Sun, W., Lal, P., 2002. Recent development on computer aided tissue engineering—a review. Comput. Methods Programs Biomed. 67, 85–103.

Tanaka, Y., Yamaoka, H., Nishizawa, S., Nagata, S., Ogasawara, T., Asawa, Y., Fujihara, Y., Takato, T., Hoshi, K., 2010. The optimization of porous polymeric scaffolds for chondrocyte/atelocollagen based tissue-engineered cartilage. Biomaterials 31, 4506–4516.

Temple, J.P., Hutton, D.L., Hung, B.P., Huri, P.Y., Cook, C.A., Kondragunta, R., Jia, X., Grayson, W.L., 2014. Engineering anatomically shaped vascularized bone grafts with hASCs and 3D-printed PCL scaffolds. J. Biomed. Mater. Res. - Part A 102, 4317–4325. doi:10.1002/jbm.a.35107

Teo, W., He, W., Ramakrishna, S., 2006. Electrospun scaffold tailored for tissue specific extracellular matrix. Biotechnol. J. 1, 918–929.

Tian, X.Y., Li, M.G., Cao, N., Li, J.W., Chen, X.B., 2009. week 2- Characterization of the flow behavior of alginate/hydroxyapatite mixtures for tissue scaffold fabrication. Biofabrication 1, 1–8. doi:10.1088/1758-5082/1/4/045005

Wang, M., Zhai, P., Chen, X., Schreyer, D.J., Sun, X., Cui, F., 2011. Bioengineered scaffolds for spinal cord repair. Tissue Eng. Part B Rev. 17, 177–194.

Wang, X., 2015. Drug delivery design for regenerative medicine. Curr. Pharm. Des. 21, 1503.

Wang, X., Ao, Q., Tian, X., Fan, J., Wei, Y., Hou, W., Tong, H., Bai, S., 2016. 3D bioprinting

technologies for hard tissue and organ engineering. Materials (Basel). 9, 1–23. doi:10.3390/ma9100802

Wang, X., He, K., Zhang, W., 2013. Optimizing the fabrication processes for manufacturing a hybrid hierarchical polyurethane–cell/hydrogel construct. J. Bioact. Compat. Polym. 28, 303–319.

Wang, X., Huang, Y., Liu, C., 2015. A combined rotational mold for manufacturing a functional liver system. J. Bioact. Compat. Polym. 30, 436–451.

Wang, X., Paloheimo, K.-S., Xu, H., Liu, C., 2010. Cryopreservation of cell/hydrogel constructs based on a new cell-assembling technique. J. Bioact. Compat. Polym. 25, 634–653.

Wang, X., Xu, H., 2010. Incorporation of DMSO and dextran-40 into a gelatin/alginate hydrogel for controlled assembled cell cryopreservation. Cryobiology 61, 345–351.

Wang, X., Yan, Y., Pan, Y., Xiong, Z., Liu, H., Cheng, J., Liu, F., Lin, F., Wu, R., Zhang, R., 2006. Generation of three-dimensional hepatocyte/gelatin structures with rapid prototyping system. Tissue Eng. 12, 83–90.

Wen, J.H., Vincent, L.G., Fuhrmann, A., Choi, Y.S., Hribar, K.C., Taylor-Weiner, H., Chen, S., Engler, A.J., 2014. Interplay of matrix stiffness and protein tethering in stem cell differentiation. Nat. Mater. 13, 979–987.

Wilson, W.C., Boland, T., 2003. Cell and organ printing 1: protein and cell printers. Anat. Rec. 272, 491–496.

Woodfield, T.B.F., Malda, J., De Wijn, J., Peters, F., Riesle, J., van Blitterswijk, C.A., 2004. Design of porous scaffolds for cartilage tissue engineering using a three-dimensional fiber-deposition technique. Biomaterials 25, 4149–4161.

Wu, W., Hansen, C.J., Aragón, A.M., Geubelle, P.H., White, S.R., Lewis, J.A., 2010. Direct-write assembly of biomimetic microvascular networks for efficient fluid transport. Soft Matter 6, 739–742.

Xu, C., Chai, W., Huang, Y., Markwald, R.R., 2012. Scaffold-free inkjet printing of three-dimensional zigzag cellular tubes. Biotechnol. Bioeng. 109, 3152–3160.

Xu, M., Van, Y., Liu, H., Yag, R., Wang, X., 2009. Controlled adipose-derived stromal cells differentiation into adipose and endothelial cells in a 3D structure established by cell-assembly technique. J. Bioact. Compat. Polym. 24, 31–47.

Xu, M., Wang, X., Yan, Y., Yao, R., Ge, Y., 2010. An cell-assembly derived physiological 3D model of the metabolic syndrome, based on adipose-derived stromal cells and a gelatin/alginate/fibrinogen matrix. Biomaterials 31, 3868–3877.

Xu, T., Binder, K.W., Albanna, M.Z., Dice, D., Zhao, W., Yoo, J.J., Atala, A., 2012. Hybrid printing of mechanically and biologically improved constructs for cartilage tissue engineering applications.

Biofabrication 5, 15001.

Xu, T., Zhao, W., Zhu, J.-M., Albanna, M.Z., Yoo, J.J., Atala, A., 2013. Complex heterogeneous tissue constructs containing multiple cell types prepared by inkjet printing technology. Biomaterials 34, 130–139.

Xu, W., Wang, X., Yan, Y., Zheng, W., Xiong, Z., Lin, F., Wu, R., Zhang, R., 2007. Rapid prototyping three-dimensional cell/gelatin/fibrinogen constructs for medical regeneration. J. Bioact. Compat. Polym. 22, 363–377.

Xu, Y., Wang, X., 2015. Application of 3D biomimetic models in drug delivery and regenerative medicine. Curr. Pharm. Des. 21, 1618–1626.

Yan, J., Huang, Y., Chrisey, D.B., 2012. Laser-assisted printing of alginate long tubes and annular constructs. Biofabrication 5, 15002.

Yan, Y., Wang, X., Pan, Y., Liu, H., Cheng, J., Xiong, Z., Lin, F., Wu, R., Zhang, R., Lu, Q., 2005a. Fabrication of viable tissue-engineered constructs with 3D cell-assembly technique. Biomaterials 26, 5864–5871.

Yan, Y., Wang, X., Xiong, Z., Liu, H., Liu, F., Lin, F., Wu, R., Zhang, R., Lu, Q., 2005b. Direct construction of a three-dimensional structure with cells and hydrogel. J. Bioact. Compat. Polym. 20, 259–269.

Yang, J., Zhang, Y.S., Yue, K., Khademhosseini, A., 2017. Cell-laden hydrogels for osteochondral and cartilage tissue engineering. Acta Biomater. 57, 1–25. doi:10.1016/j.actbio.2017.01.036

Yeo, M., Lee, H., Kim, G.H., 2016. Combining a micro/nano-hierarchical scaffold with cell-printing of myoblasts induces cell alignment and differentiation favorable to skeletal muscle tissue regeneration. Biofabrication 8, 35021.

You, F., Wu, X., Chen, X., 2016a. 3D Printing of Porous Alginate/gelatin Hydrogel Scaffolds and Their Mechanical Property Characterization. J. Int. J. Polym. Mater. Polym. Biomater. 66, 299–306. doi:10.1080/00914037.2016.1201830

You, F., Wu, X., Zhu, N., Lei, M., Eames, B.F., Chen, X., 2016b. 3D Printing of porous cell-laden hydrogel constructs for potential applications in cartilage tissue engineering. ACS Biomater. Sci. Eng. 2, 1200–1210.

Yu, Y., Zhang, Y., Martin, J.A., Ozbolat, I.T., 2013. Evaluation of cell viability and functionality in vessel-like bioprintable cell-laden tubular channels. J. Biomech. Eng. 135, 91011.

Yu, Y., Zhang, Y., Ozbolat, I.T., 2014. A Hybrid Bioprinting Approach for Scale-Up Tissue Fabrication. J. Manuf. Sci. Eng. 136, 61013. doi:10.1115/1.4028511

Zehnder, T., Sarker, B., Boccaccini, A.R., Detsch, R., 2015. Evaluation of an alginate-gelatine crosslinked hydrogel for bioplotting. Biofabrication 7. doi:10.1088/1758-5090/7/2/025001

Zhang, T., Yan, Y., Wang, X., Xiong, Z., Lin, F., Wu, R., Zhang, R., 2007. Three-dimensional gelatin and gelatin/hyaluronan hydrogel structures for traumatic brain injury. J. Bioact. Compat. Polym. 22, 19–29.

Zhang, Y., Yu, Y., Ozbolat, I.T., 2013. Direct bioprinting of vessel-like tubular microfluidic channels. J. Nanotechnol. Eng. Med. 4, 20902.

Zhang, Y.S., Khademhosseini, A., 2015. Seeking the right context for evaluating nanomedicine: from tissue models in petri dishes to microfluidic organs-on-a-chip. Nanomedicine 10, 685–688.

Zhang, Y.S., Oklu, R., Dokmeci, M.R., Khademhosseini, A., 2017. Three-Dimensional Bioprinting Strategies for Tissue Engineering. Cold Spring Harb. Perspect. Med. a025718. doi:10.1101/cshperspect.a025718

Zhang, Z., Wang, B., Hui, D., Qiu, J., Wang, S., 2017. 3D bioprinting of soft materials-based regenerative vascular structures and tissues. Compos. Part B Eng.

Zhao, X., Liu, L., Wang, J., Xu, Y., Zhang, W., Khang, G., Wang, X., 2014. In vitro vascularization of a combined system based on a 3D printing technique. J. Tissue Eng. Regen. Med.

Zhao, X., Wang, X., 2013. Preparation of an adipose-derived stem cell/fibrin–poly (d, l-lactic-co-glycolic acid) construct based on a rapid prototyping technique. J. Bioact. Compat. Polym. 28, 191–203.

Zhou, X., Zhou, X., Liu, C., Wang, X.H., 2016. A 3D bioprinting liver tumor model for drug screening. World J. Pharm. Pharm. Sci.

Zhu, W., Ma, X., Gou, M., Mei, D., Zhang, K., Chen, S., 2016. 3D printing of functional biomaterials for tissue engineering. Curr. Opin. Biotechnol. 40, 103–112. doi:10.1016/j.copbio.2016.03.014

Zopf, D.A., Hollister, S.J., Nelson, M.E., Ohye, R.G., Green, G.E., 2013. Bioresorbable airway splint created with a three-dimensional printer. N. Engl. J. Med. 368, 2043–2045.

Figure captions

Figure 1. Schematic of a) inkjet-based, b) laser-based, and c) dispensing-based machines

Figure 2. Different types of dispensing-based bioprinting techniques: positive displacement, time pressure, and rotary screw approaches

Figure 3. Schematic of the fabrication process of a hybrid ear-shaped scaffold by a dispensing-based 3D bioprinting technique including I) conversion of the medical image to a CAD model, II) transformation of the data to the machine, III) biomaterial and cell source selection, and IV) bioprinting of sacrificial support, auricular cartilage, and fat tissue

Figure 4. The evolution of complex organ manufacturing based on hybrid scaffolds using medical imaging

Figure 5. 3D biprinting of complex structures via sacrificial support for ear regeneration: a) obtaining CAD model from imaging data, b) left picture: 1- converting CAD model to STL file, 2- investigation of the accuracy of STL file, 3- defining desired parts for bioprinintg with different cells, 4- creation of the CAD model of sacrificial support based on main CAD model, 5- fabrication of porous scaffold via bioprinter, right picture: a representative sample of ear fabricated by a 3D-Bioplotter (CAD model is available at https://www.thingiverse.com/thing:304657 (Addamay123, 2017))

Figure 6. Printing of vascular networks within hybrid scaffolds using: a) hydrogel reservoir, b) coaxial nozzle, c) sacrificial material: I) CAD models of main (hybrid biomaterials) and sacrificial parts, II) final scaffold before removing sacrificial material (inset is the top view during fabrication), III) final hybrid scaffold after removal of the sacrificial material

Tables

Table 1. Merits and demerits of common 3D bioprinting techniques

Table 2. Potential biomaterials and printing parameters used in the biofabrication of hybrid scaffolds

Table 3. Physical architecture and mechanical properties of hybrid scaffolds

Table 4. Printing parameters and reported cell viability for different kinds of cells